Technical report; TR-229

KNMI

Evaluation of humidity and temperature measurements of Vaisala's HMP243 plus PT100 with two reference psychrometers

E.M.J. Meijer

Koninklijk Nederlands Meteorologisch Instituut

De Bilt, 2000

Technical report = Technisch rapport; TR-229

De Bilt, 2000

PO Box 201
3730 AE De Bilt
Wilhelminalaan 10
Telephone +31 30 220 69 11
Telefax +31 30 221 04 07

Author: E.M.J. Meijer

UDC: 551.508.71

ISSN: 0169-1708

ISBN: 90-369-2185-6

Evaluation of humidity and temperature measurements of Vaisala's HMP243 plus PT100 with two reference psychrometers.

November 2000

E.M.J. Meijer

Contents

1. Introduction

The 213 m meteorological tower Cabauw near Utrecht, used for experimental boundary layer research has been renovated and became operational in 2000 for new observational programs. In the past the tower was meanly used for atmospheric research programs and temperature and humidity profiles were measured with dry- and wet bulb psychrometers (Assmann-type) at 20 m intervals.
In the near future the tower will be run as a synoptic/experimental station. For this and reasons of easier maintenance and standardization, the tower is equipped at several levels with a new relative humidity (RH) sensor; HMP243 in a Vaisala screen and next to it a temperature sensor; PT100 in a standard KNMI screen.
The capacitive RH sensor is, when compared to the "old" HMP233, believed to be faster in response and more reliable under difficult conditions like RH > 90% and mist (See TR-201 KNMI, F. Kuik, de Bilt, 1997).
Determination of humidity and temperature profiles of the boundary layer for Atmospheric Research, demand higher specifications then synoptical observations, due to the very small differences at the different intervals. Doubts rose about these sensors if they could meet the higher expectations. From experience and literature (G. Lefebvre, T. Anderson and I. Mattisson, TECO, 1998) it is known that these measurements can be influenced by the sensor shield or screen and by various meteorological conditions.

Expectations
Because the different mechanical and physical characteristics of the HMP243 (+ PT100) compared to the psychrometer, there are reasons to belief that there would be noticeable effects on the measurements caused by radiation, wind, precipitation and dew on the screens.
- Radiation effects like heating and cooling of the screen during the day respectively night.
- Lagging of temperature and humidity signals during periods of low wind speed.
- Cooling effects through evaporation of dew or precipitation on the outside of the screen.
- Humidity effects caused by evaporation of dew on the inside of the screen.

Experimental set-up
For a correct interpretation of humidity and temperature profiles, understanding of the performance of these new sensors under various meteorological conditions was very desirable. Therefore the sensor behavior was determined in an experimental set-up.
As location we choose the experimental site of KNMI in De Bilt, for reasons like easy access for daily monitoring, control and availability of comparable instruments.
A set of instruments was set up to measure the various meteorological conditions at the test site.
Important is a reference instruments to compare the measurements with. Of course there is no absolute reference instrument for measuring humidity and temperature under field conditions but we used two sets of psychrometers, one from KNMI and one from LUW (now called Wageningen University & Research Center). Both the LUW- and KNMI instrument are considered very trustworthy and have a long measuring history. The KNMI psychrometer is extensively tested and described in a scientific report (WR78-1, W. Slob) and used in the Cabauw tower for almost 25 years (15 years measuring period).

This document describes the used material and methods plus an analysis of the measurements.

2. Material and methods

2.1 Material

At the experimental site of the KNMI, a configuration was set up to compare the data of the RH sensor + PT100 with the psychrometers, see Figure 2.1 next page.
The various instruments were attached to standard aluminum H-arms or at a pole, 1.5m. above the grass (Photo 1).

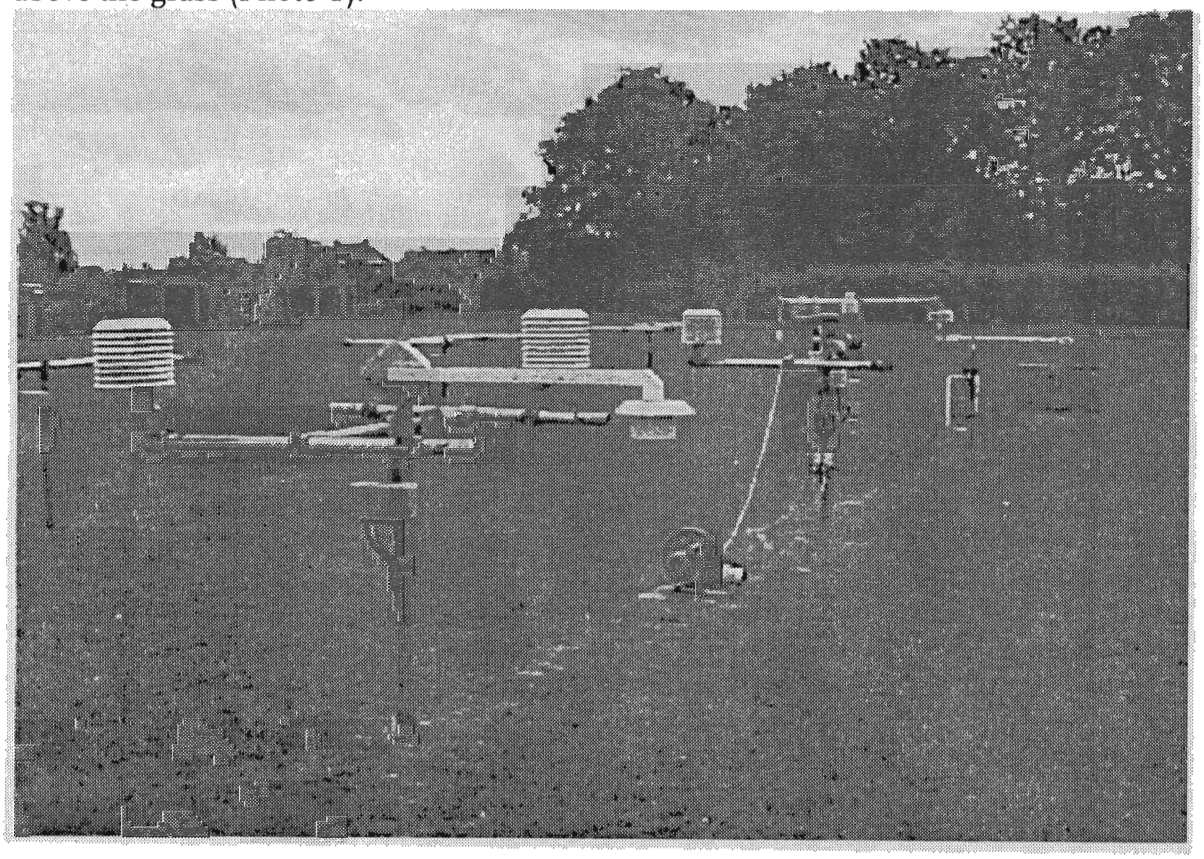

Photo 1: Experimental set-up at KNMI.

The following instruments were used for the experiment:

INSTRUMENT	QUANTITY	RESOLUTION	ACCURACY
Schulze radiometer + PT100	NET radiation ↓↑	1 W/m²	± 1% or 5 W/m²
KNMI PT500 psychrometer	Tdry & Twet	0.01 °C	± 0.1°C
LUW PT100 psychrometer	Tdry & Twet	0.01°C	± 0.1°C
KNMI dew sensor	Dew	wet/dry	wet/dry
Vaisala HMP243	Tdew (+Tamb⇒RH)	0.5 % RH	± 0.5 + 2.5% x fraction(RH)
Vaisala PT100	Tdry	0.01°C	± 0.1°C
Kipp CM11 pyranometer *	Global radiation ↓	1 W/m²	± 1% or 3 W/m²
Kipp CM11 + shadow ball *	Diffuse radiation ↓	1 W/m²	± 1% or 3 W/m²
Kipp CM11 pyrheliometer *	Direct radiation ↓	1 W/m²	± 1% or 3 W/m²
KNMI cup anemometer	Wind speed 1.5 m.	0.06 m/s	0.5 m/s
Present Weather sensor	Precipitation	PW-code	-

* All Kipp CM11 were mounted on an automatic sun tracker.

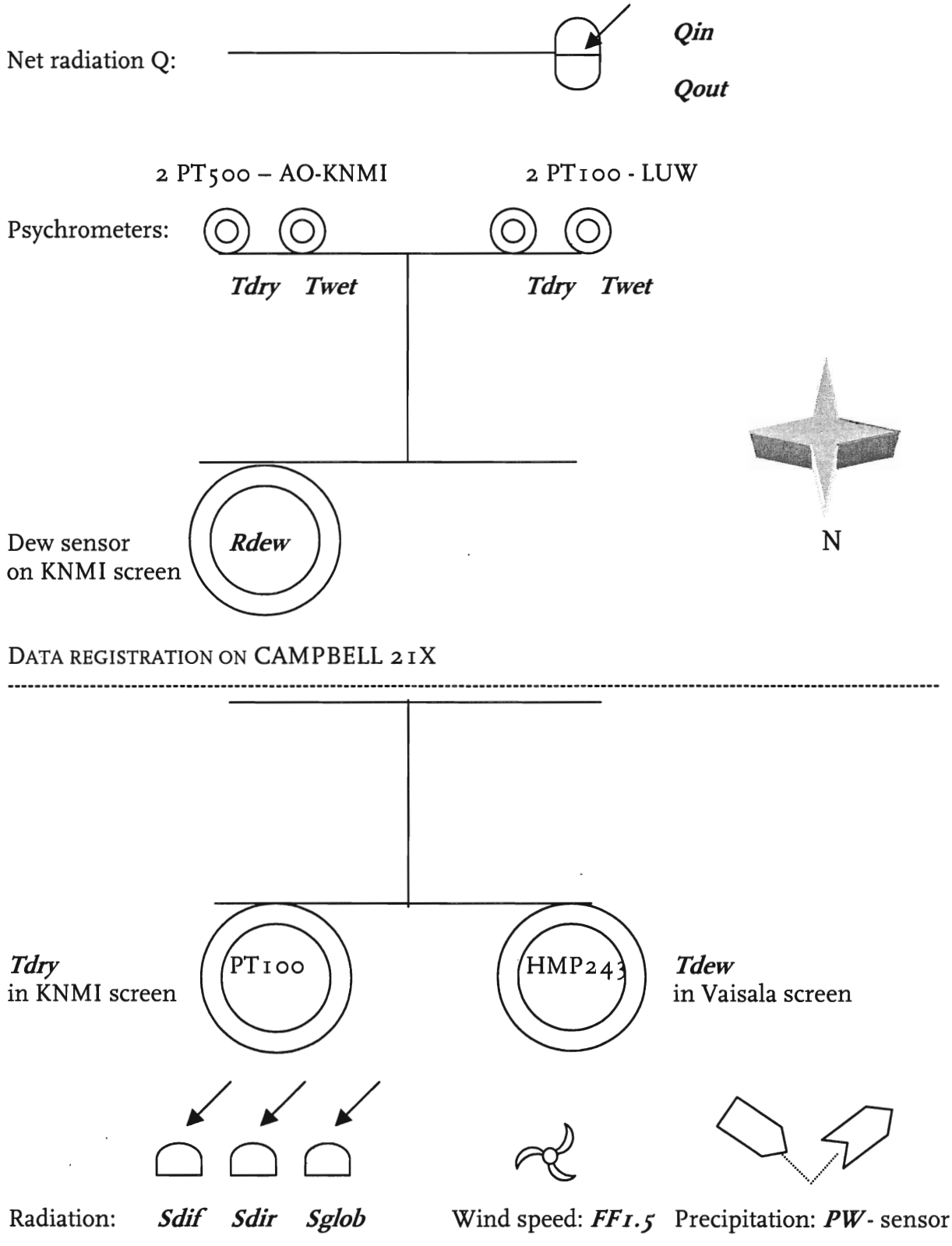

Figure 2.1 KNMI experimental site description

2.1.1 Schulze radiometer.

The NET radiation (0.3 – 100 μm) was measured with a Schulze radiometer (Photo 2). It consisted of two half domes, one looking upward and one looking downward. The domes were made of thin self-supporting poly-ethylene. The instrument was attached to a long (spirit level) boom, so the downward looking radiometer did not see the vertical mounting pole. The domes were externally ventilated to keep them reasonably free from dew and precipitation.
The principle of measurement is based on the difference in temperature over the thermopile in the domes, caused by the radiation.
Next to the thermopile measurements, the body temperature of the Schulze was measured with a PT-element.
The calibration curve of the PT100 is shown in appendix A1 and was performed on 7-5-1999 by the KNMI calibration laboratory.

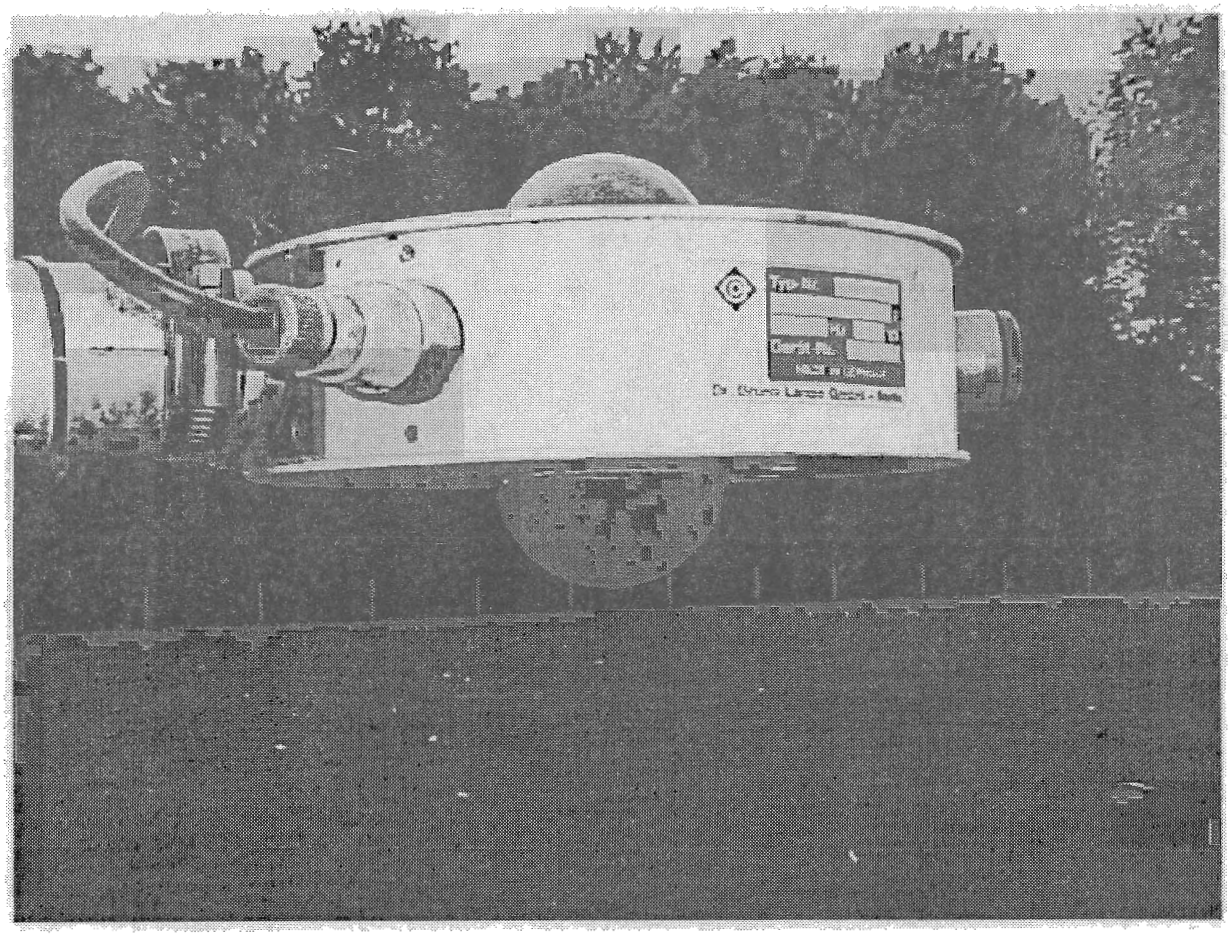

Photo 2: Schulze radiometer.

2.1.2 KNMI PT500 Psychrometer

The psychrometer was developed at KNMI (AO division) according to the model that served in the mast of Cabauw from 1972 to 1997. The main difference with this older model is that the thermocouples were replaced with PT500 elements and that the inside of the inner cylinder was slightly increased to prevent forming of a water bridge with the slightly bigger thermometer element (Photo 3).
The PT-elements for measuring dry and wet bulb temperature were actually inside two separate ventilated and shielded cylinders (W.H. Slob, WR78-1).
A ventilation speed has been chosen that keeps the air speed within the shield independent of the wind speed. The best value was found to be 6 m/s. A robust 220V Stefan ventilator was used.
The wet bulb sleeve was kept wet with a peristaltic water pump, there was no extra suction to remove superfluous water. This water hung at the end of the wet bulb in an equilibrium between gravity and upward ventilation stream, until it was taken upwards.
The calibration curve of the PT500 is shown in appendix A2 and was performed on 7-5-1999 by the KNMI calibration laboratory.

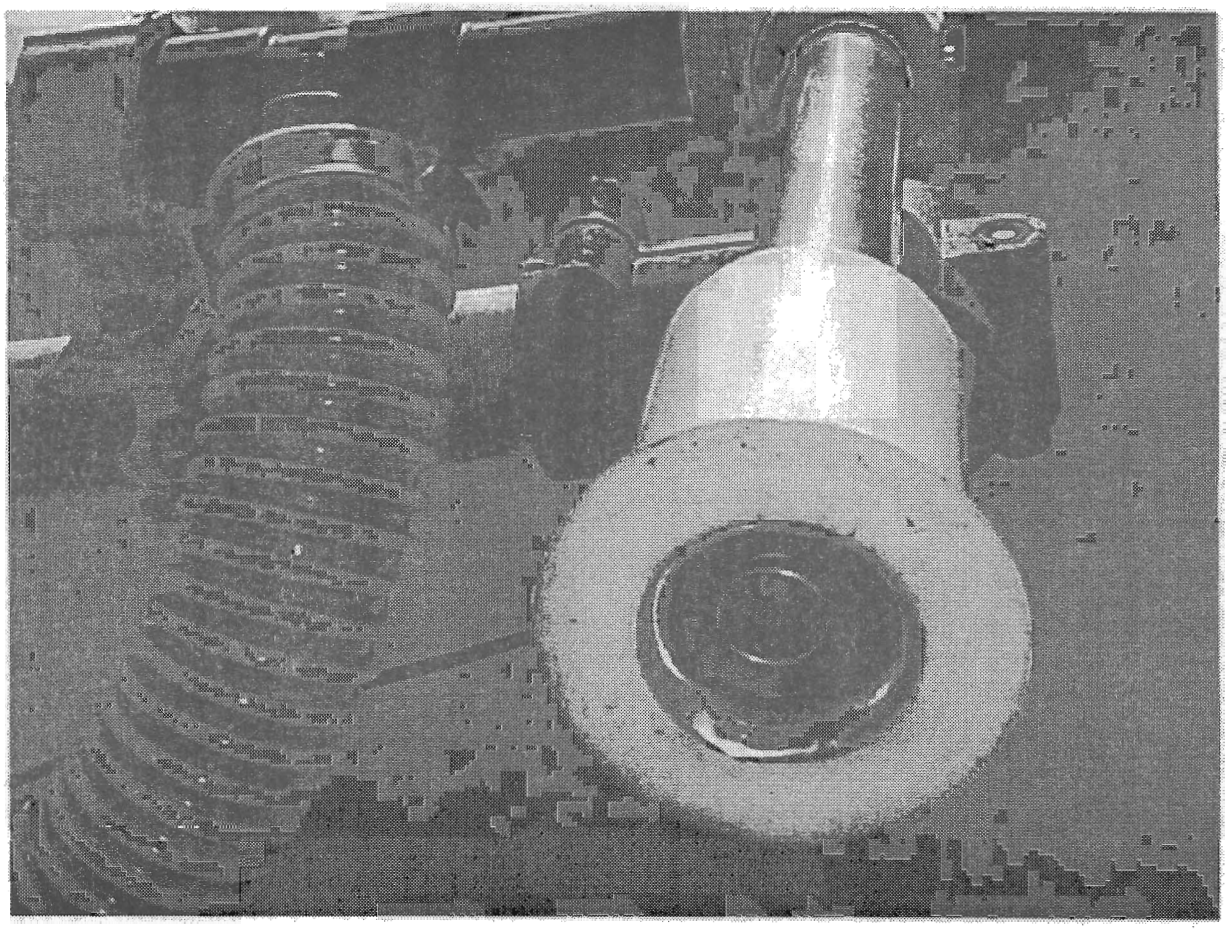

Photo 3: KNMI PT500 Psychrometer (Only wet bulb).

2.1.3 LUW PT100 Psychrometer

This instrument was developed by the LUW. The psychrometer differs from the KNMI type mainly in three ways;

- It has a cup-screen-like cylindrical construction that holds the ventilator plus two double shielded hollow pipes, sticking out the bottom of the cylinder and isolating the PT100's from radiation.
- The ventilation speed in the hollow pipes shielding the PT-elements, is much lower than that of the KNMI PT-elements.
- It has a vacuum pump for the suction of superfluous water at the end of the sleeve of the wet bulb.

Especially this last feature has caused some problems in the beginning of the experiment.
- First of all, the distance between the adjustable small suction-pipe and the wet bulb sleeve was critical;
When too large; superfluous water introduced a thermal bridge between inner shield and PT-element: causing an overestimation of Twet.
Too narrow, introduced a thermal bridge between suction-pipe and PT-element: ⇒ ditto.
- Secondly the voltage of the suction pump appeared to be a little too low for continuous operation. After we increased it from 10 to 12V the problem did occur no more.

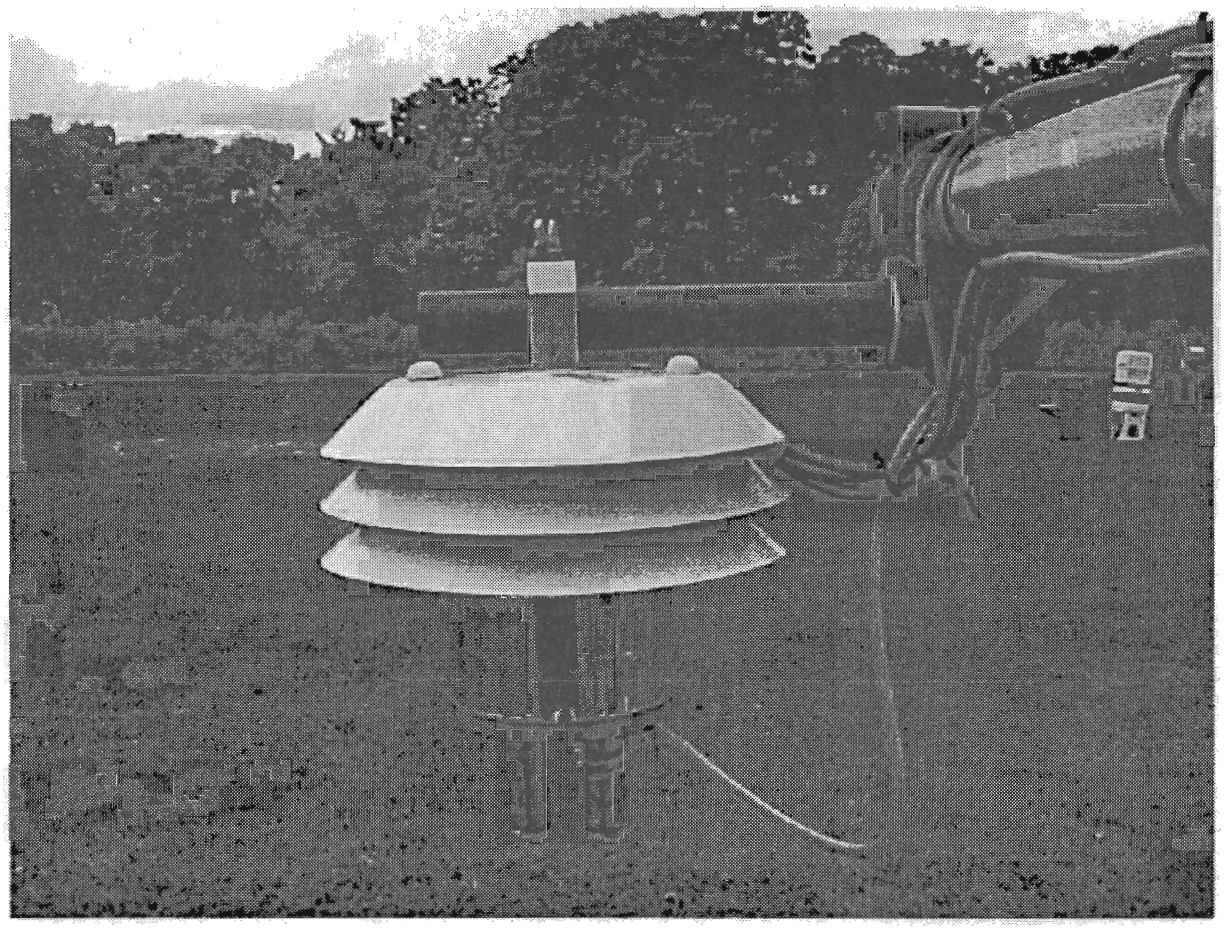

Photo 4: LUW PT100 Psychrometer

2.1.4 KNMI dew sensor

To take into account the cooling effect of the screens caused by evaporation of moisture on the screens, an instrument was needed that could detect the existence of moisture, dew or rain on the surface of the screens.
There is hardly any dew sensor on the commercial market, because it is very difficult to develop a sensor that doesn't influence the characteristics of the material it is mounted on.
So the development of dew sensors can not be seen independent of the surface material under investigation and is therefore commercially not very interesting.

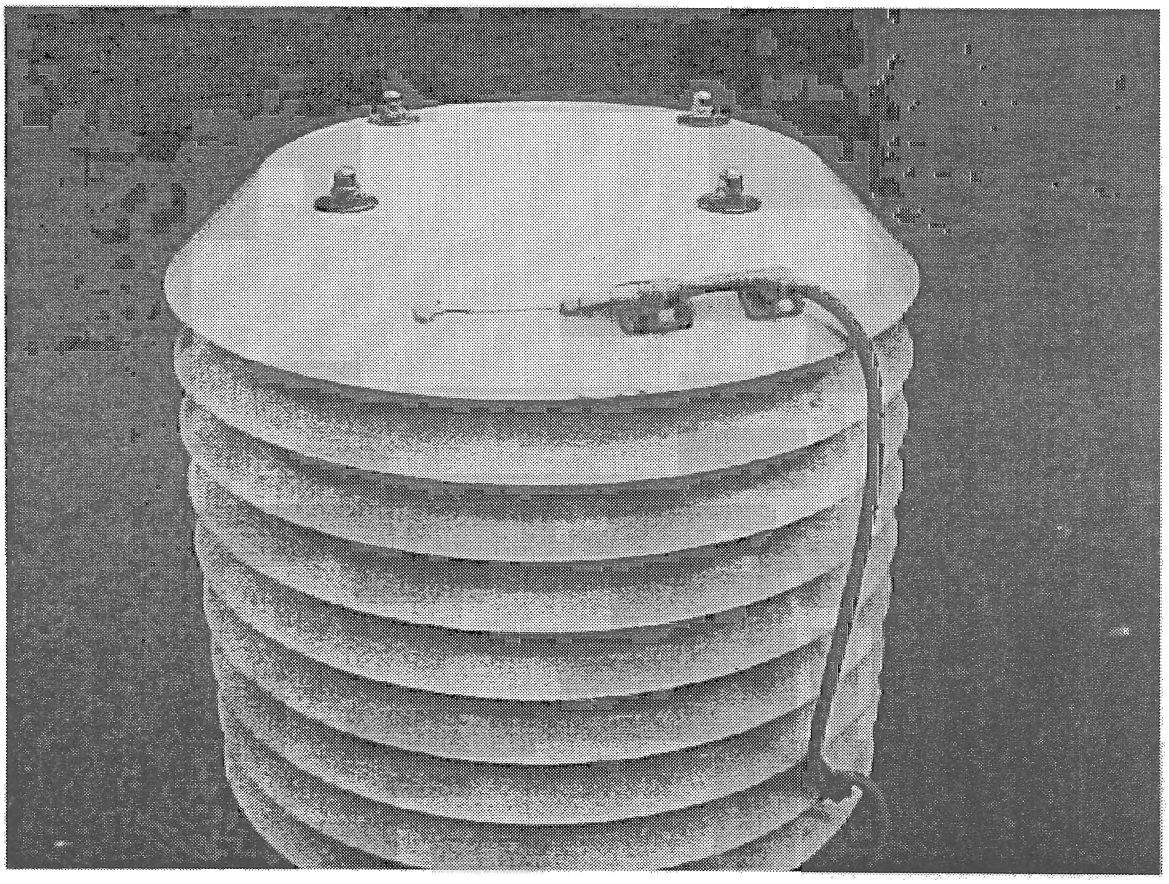

Photo 5: KNMI Dew sensor on standard KNMI screen.

That is why we developed a simple dew sensor ourselves that wouldn't influence dew forming on the surface of a standard KNMI screen.
It basically consisted of two parallel silver wires that were fixed in place on the surface. The sensor was constructed so that the thin wires just didn't make contact and so were able to detect the smallest possible droplets or dew.
It proved to be working well.
In situations where the PW-sensor didn't detect any form of precipitation, the dew sensor was capable of detecting dew forming during periods of high humidity especially in the morning (See figure 2.2). It also detected the wet state of a screen long after a period of rain.

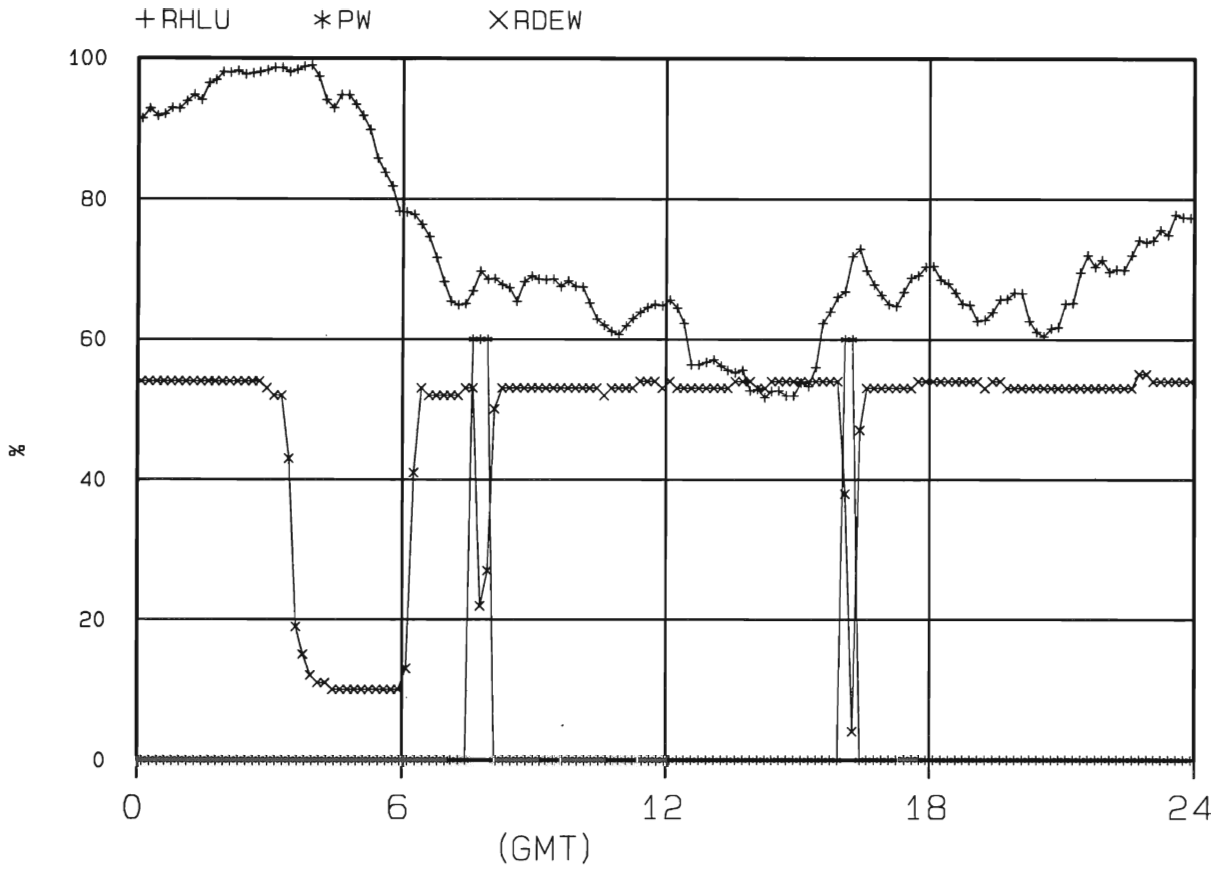

Figure 2.2: *Response of dew sensor (dew if Rdew = [0–40], dry if Rdew = [40–60]). Dew sensor clearly detects dew or wet surface after long period of high humidity or rain on 19/7/99 (Precipitation; then PW-code > 0).*

2.1.5 Vaisala HMP243 + PT100

The RH sensor HMP243 is the sensor under test and therefore discussed more extensive than the other sensors.
The HMP243 differs a little from the HMP233, used at many AWS stations. The latter capacitive sensor directly measures relative humidity of the air, according to the humidity dependency of the diëlectricum of capacitors.
The HMP243 uses the same capacitive sensor but is heated a few degrees above ambient temperature (Tdry). Since dewpoint temperature (Tdew) is independent of Tdry, Tdew can be determined. To calculate RH, an additional measurement of Tdry is necessary with a PT100 in a nearby KNMI screen.

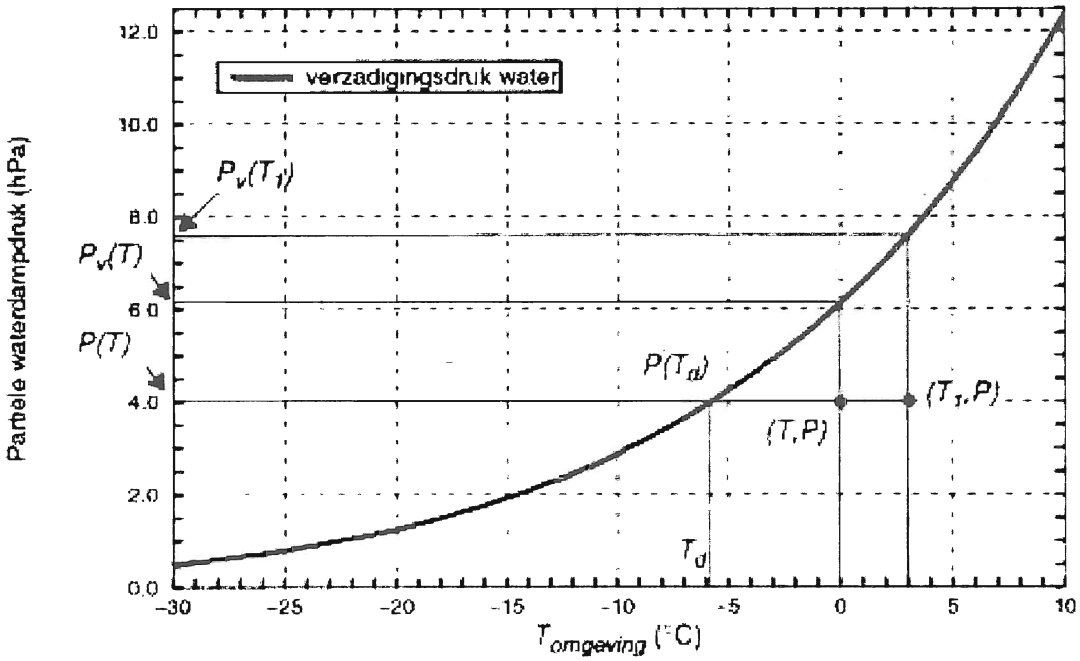

Fig. 2.3: *PT-diagram for water in relation to the determination of RH.*

The curve shows when air is saturated with water vapor by a certain combination of partial water vapor pressure *(P)* and temperature *(T)*.
Consider point *(T,P);* the saturation vapor pressure at this temperature is $P_v(T)$.

The relative humidity is defined as:

$$RH = \frac{P(T)}{P_v(T)} \bullet 100\% \qquad (2.1)$$

This is the *RH* measured by a standard HMP233. However the HMP243 doesn't measure at *T*, but at the temperature of the heated element; T_1. This results in a RH_{243} that is lower than the *RH* derived from equation (2.1) because the corresponding saturation pressure is too high:

$$RH_{243} = \frac{P(T)}{P_v(T_1)} \bullet 100\% \qquad (2.2)$$

By means of a PT-element on the RH sensor, T_1 of the sensor is measured. In equation (2.2), $P(T)$ is the only unknown factor and can be derived from the other parameters. We are not really interested in $P(T)$ but more in T_d ($=T_{dew}$) which can be derived from it. Namely $P(T) = P_v(T_{dew})$ and the relation between P_v and T_{dew} is known.

The basic quantity that the HMP243 produces is T_{dew}, which is determined according the above. If the ambient temperature *T* is not known, the HMP243 can not generate RH as output. However the HMP243 has an option to connect an external PT100 to measure the ambient temperature *T*. With this additional information HMP243 can determine the correct RH, combining equation (2.1) and (2.2):

$$RH = \frac{P_v(T_1)}{P_v(T)} \bullet RH_{243} \qquad (2.3)$$

The saturation pressure of water P_v is only a function of the temperature and well known. $P_v(T)$ and $P_v(T_1)$ are calculated, RH_{243} is measured and RH can be determined from (2.3).
The calculation of RH could be performed in the HMP243 internally, but the analog output in this experiment is configured to produce T_{dew} as output. Calculation of RH is performed in the *"Mobibase"* software (database for experimental data, Bosveld).

Vaisala's HMP243 housing is an open cylinder-like construction with one cup on top and it has no bottom plate (Photo 6). The nearby (1m) standard KNMI (multiple) cup screen holds the additional PT100 and is closed at the bottom side.

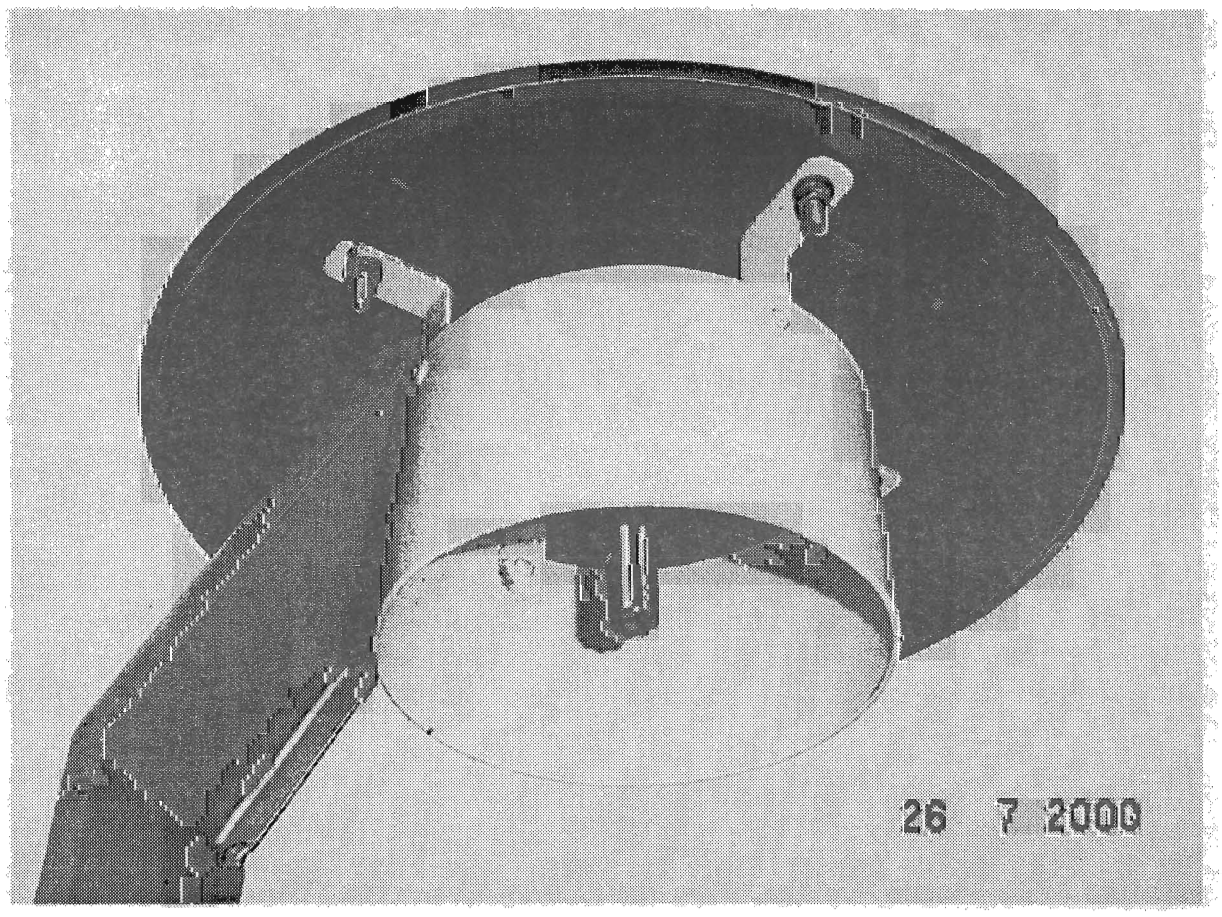

Photo 6: Vaisala HMP243 humidity sensor in Vaisala screen.

Since the other used instruments are standard operational sensors, these are not described in detail, more information about these sensors can be obtained from INSA, the Measurement and Information Systems Department at KNMI.

2.1.6 Kipp CM11 's

Radiation is measured with the standard AWS instruments. All radiometers are mounted on an automatic sun tracker.

- Global radiation (305 – 2800 nm) is measured with a Kipp CM11 pyranometer. It measures short wave radiation also known as global radiation, being the sum of direct and diffuse radiation.
- Diffuse radiation is measured with a Kipp CM11 pyranometer, equipped with a shadow ball, to exclude the direct radiation of the sun.
- Direct radiation is measured with a Kipp pyrheliometer.

2.1.7 KNMI cup anemometer

The local wind speed at the experimental site is measured with a standard cup anemometer. The digital anemometer is positioned approximately 3m North from the Vaisala screen on a pole, 1.5 m above grass level. (Before 5/7/99 no FF1.5 was available, readings came from the standard wind meter at the 18m tower.)
The measurement is based on a frequency measurement. A combination of a LED and light sensitive detector (opto-coupler), separated by a rotating disc with gaps, counts the number of rotations per time unit.

1.1.8 Present Weather sensor

The Present Weather sensor gives information about the kind of precipitation. The sensor consists of an optical transmitter and receiver. The back scatter signal, reflected by the particles in the optical path, is characterized by the shape of the particles and thus by the character of precipitation.
The table explains the generated PW-code;

Kind of PRECIPITATION	PW-code
No precipitation	00
Precipitation	40
Drizzle	50
Cooled drizzle	55
Rain and drizzle	57
Rain	60
Cooled rain	65
Rain and snow	67
Snow	70
Ice rain	75
Sleet	77
Ice crystals	78
Grainy snow and –hail	87
Hail	89

2.2 Methods

Evaluation of the performance of the HMP243 and PT100 under various meteorological conditions, raised the need for a reference to compare the measurements with.

Therefore two sets of psychrometers were set up as reference instruments near the HMP243 and PT100. One modified KNMI- model and another slightly different constructed psychrometer was borrowed from LUW (B. Heusinkveld). One reason for using two psychrometers was minimizing the risk of failure. Another reason for the duplo set up was that the consistency and mutual behavior of two different psychrometers could be studied.

Furthermore sensors were set up at the KNMI experimental site that would record the various meteorological conditions that could influence the humidity and temperature measurement of the HMP243 and PT100.
Data of standard AWS (Automatic Weather Station)-sensors were recorded by KNMI SIAM's (Sensor Intelligente Aanpassings Module) and data of non-standard sensors were recorded by a Campbell 21X - datalogger. See chapter 2.2.2.

The experiment was performed over a period of 6 months from summer (June) until early frost (November), to cover a large variety of meteorological conditions.
Frost in November brought limitations to measurements with (wet bulb) psychrometers and therefore limited the continuity of the comparison.

2.2.1 AWS – data handling

Data of the standard sensors (Vaisala's, Kipp CM11, cup anemometer and PW-sensor) were registered by the SIAM of AWS-261 and AWS-262 (Radiation).
A SIAM is an independently operating unit that can be regarded as an intelligent interface between the meteorological sensor and the data handling system (AWS). Output of the SIAM is independent of the particular sensor used in order to obtain a modular set up of the measuring system.
Thus new generation sensors can be used without extensive modification of the measuring system. The 10-minute averages were calculated from 50 values, measured every 12 seconds.

Data of the AWS was checked for discontinuities and mailed by A. Mazee (INSA) to E. Meijer (AO).
These rh<weeknr>.DAT files were saved to local disc (C:\vergex\AWSdata) for backup and saved to a shared disc (J:\ks-ao\mobibase\vergex\dat) for common use in database programs.
The MOBIBASE software package was developed (F. Bosveld, KNMI) for graphical and statistical interpretation and comparison of micro-meteorological observations from different sources and different data file formats. For a description of the package see also http://info.knmi.nl/~bosveld/mobibase/mobibase.htm

With the program "TRANSFER", columns of external AWS-data files (.DAT) were added to the MOBIBASE database with the .A10 - extension (10 minute averages).

2.2.2 21X datalogger – data handling

The data of the non-standard instruments (Schulze, 2 psychrometers and dew sensor) were registered by a Campbell 21X data logger with multiplexer. A special 21X-program (psych.doc) was written to read in all the sensor signals from the instruments. In the program all calibration curves of the used PT-elements were entered to calculate the exact values. Every week data from the data logger was offloaded on site with a laptop and copied to PC on local disc (C:\vergex) for backup.
A DOS application SPLIT.COM converted the 21X-files into print files with the data nicely split into columns. These output files (PS<yymmdd>.PRN) were copied to shared disc (J:\ks-ao\mobibase\vergex\dat) for common use in database programs.
With the program "DATATRNS" in MOBIBASE, data and calculated derived quantities were converted into a special format for interpretation in MOBIBASE.

A copy of the data set was made in which unreliable data, like e.g. wet bulb temperature during a failure of the water pump, were excluded. All analysis is performed on this cleaned data set ("ve<yyyymmdd>.B10" -files). For all interpretation 10 minute averages (instead 30 or 60 min.) were used, that on one hand keep reasonably track of variations and on the other hand keep data amounts manageable.

In appendix A4the acronym description is given of all measured and derived variables used in the Mobibase program and throughout this document.

Equations used for derived quantities of variables measured with the 21X.

In the Mobibase program several subroutines were used for calculation of the derived quantities. TdewAO, TdewLU, RHAO, RHLU, RHAW, TwetAW, Qinc, Qoutc and Qnet were calculated according these equations.

TdewAO and TdewLU
The saturated vapour pressure for T ≥ 0 °C can be calculated as:

$$Esat(T) = 6.11213 \bullet e^{\frac{17.50 \bullet T}{241.2+T}} \quad \text{(mbar)} \qquad (2.4a)$$

where 6.11213 is the saturated vapour pressure for T=0 °C ,
and for T< 0°C:

$$Esat(T) = 6.11213 \bullet e^{\frac{22.44 \bullet T}{272.18+T}} \quad \text{(mbar)} \qquad (2.4b)$$

Epsych is derived from the psychrometer equation, where $\gamma = 6.460 \cdot 10^{-4}$ ($°C^{-1}$) is the psychrometer constant and P is the air pressure:

$$Epsych = Esat(Twet) - \gamma \bullet P(Tdry - Twet) \qquad \text{(mbar)} \qquad (2.5)$$

Combining (2.4) and (2.5) gives the dewpoint temperature TdewAO or TdewLU, for Epsych ≥ 6.11213 :

$$Tdew_{ao/lu} = \frac{241.2}{\left(17.50 / \ln(Epsych/6.11213)\right) - 1} \quad (°C) \quad (2.6a)$$

and for Epsych <6.11213:

$$Tdew_{ao/lu} = \frac{272.18}{\left(22.44 / \ln(Epsych/6.11213)\right) - 1} \quad (°C) \quad (2.6b)$$

RHAO and RHLU

The relative humidity RHAO and RHLU were derived from equation (2.4) and (2.5):

$$RH_{ao/lu} = 100\% \bullet \frac{Epsych(Tdry, Twet, P)}{Esat(Tdry)} \quad (\%) \quad (2.7)$$

RHAW

From the AWS sensor HMP243 and a separate PT100-element we got Tdew and Tdry as output, RHAW and TwetAW were derived as follows:

$$RH_{aw} = 100\% \bullet \frac{Esat(Tdew_{aw})}{Esat(Tdry_{aw})} \quad (\%) \quad (2.8)$$

TwetAW

As Twet can not be defined directly as function of Esat and Tdry , it was calculated in a Newton-Rapson iteration until $\Delta T < 0.001$ °C. $\gamma = 6.460 \cdot 10^{-4}$ (°C^{-1})
Therefore we first had to define an Esat derivative; dEsat/dT:

For T ≥ 0°C:
$$\frac{dEsat(T)}{dT} = Esat(T) \bullet \frac{4222.0}{(241.2 + T)^2} \quad (g.kg^{-1}.K) \quad (2.9)$$

For T < 0°C:
$$\frac{dEsat(T)}{dT} = Esat(T) \bullet \frac{6108.8}{(272.18 + T)^2} \quad (g.kg^{-1}.K) \quad (2.10)$$

Iterative
$$Twet_{aw} = Twet_{old} - \frac{(Epsych(Tdry, Twet_{old}, P) - Esat(Tdew))}{\left(\frac{dEsat}{dT}\right)_{Twet_{old}} + \gamma \bullet P} \quad (°C) \quad (2.11)$$

Qinc, Qoutc, Qnet

The incoming (↓) and outgoing (↑) total radiation measured by the dual-dome Schulze NET radiometer need to be incremented with the black body radiation of the housing. Moreover a correction for the different sensivity of the instrument for longwave and shortwave radiation has to be applied.

For correction the following constants were used:

Albedo grass $\alpha = 0.23$
Stefan-Bolzman constant $\sigma = 5.67 \times 10^{-8}$ ($W.m^{-2}.K^{-4}$)
Qin calibration factor Ci = 0.035 (Kohsiek)
Qout calibration factor Co = 0.048 (Kohsiek)

From $Qin_{schulze}$, measured with the upper thermopile sensor, the incoming radiation Qinc is calculated as follows:

$$Qinc = Qin_{schulze} - Ci \bullet Sglob + \sigma \bullet T_{house}^{4} \qquad (W.m^{-2}) \qquad (2.12)$$

where Sglob is the global radiation measured by the AWS sensor.

From $Qout_{schulze}$, measured with the lower thermopile sensor, the outgoing radiation was calculated in a similar way:

$$Qoutc = Qout_{schulze} - Co \bullet \alpha \bullet Sglob + \sigma \bullet T_{house}^{4} \qquad (W.m^{-2}) \qquad (2.13)$$

Then finally the NET radiation was calculated from the difference between the corrected incoming and outgoing radiation:

$$Qnet = Qinc - Qoutc \qquad (W.m^{-2}) \qquad (2.14)$$

2.2.3 Synchronisation data acquisition

In order to interpret the differences of the absolute signal levels, we must be sure that these signals show no difference in phase caused by an asynchronous data acquisition. Because two different data acquisition systems were used (AWS and 21X), synchronisation in time is important.
At regular intervals (2 – 4 weeks) the AWS-time was synchronised with the DCF clock of a computer, the AWS clock always showed a deviation of less than 30 seconds. The internal 21X-clock was also checked with this DCF clock and showed a deviation of less than 30 seconds after 3 months.
All data points recorded by both systems are average values over the leading 10-minutes, with the time stamp at the end of that period.
To show synchronisation between the AWS and 21X best, we have chosen two signals of a quantity (precipitation) that is not delayed by the sensor environment (like temperature in a screen).

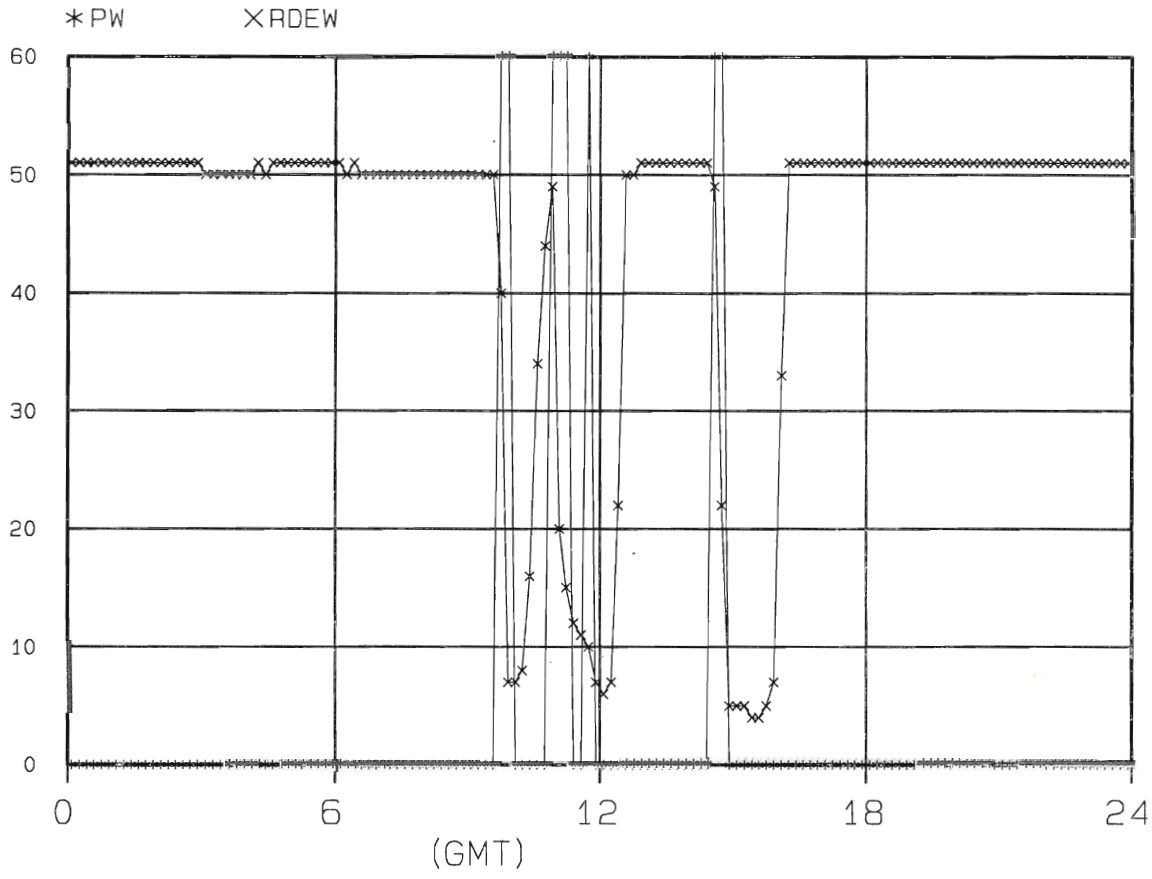

Figure 2.4 *Data synchronisation between a 21X-signal (dew) and AWS-signal (PW-code) (on 19/7/99).*

Figure 2.4 shows that the phase difference between the two signals for the precipitation can be neglected. The start of four short periods of rain, represented by the rise of the PW-code (AWS), is instantaneously followed by the drop of the dew signal (21X).
(The dew signal also shows how long the screen stayed wet.)

3. Results

This chapter describes the results of the comparison of the different sensors.
In chapter 3.1 a mutual comparison between the measurements of the two psychrometers is discussed to determine the reference instrument for further comparison.
In chapter 3.2 measurements of the AWS-sensors under test; HMP243 and the PT100 are compared with measurements of the reference instrument.

3.1 Comparison of LU- and AO-psychrometer measurements

Because the measurements were performed with two psychrometers, it was necessary to determine which of the two could best be referred to as the reference instrument. The aim was to compare the AWS-sensors with only one instrument instead of two.
Tdry and Twet were the best parameters to test this because they were measured directly by the psychrometers and not derived. To interpret the results of the two psychrometers in perspective, we also compared it with the performance of the AWS-sensors.

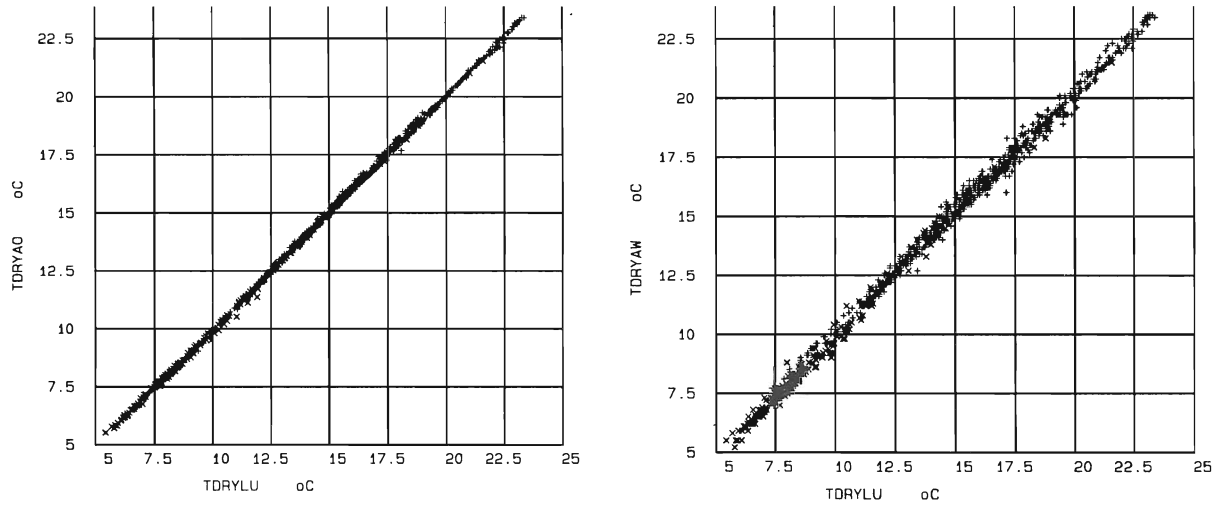

Figure 3.1: *Comparison between dry bulb temperatures; TdryLU with TdryAO (left) and TdryLU with TdryAW (right) for low(x:<1 m/s) and high(+:>1 m/s) wind speed.*

3.1.1 Dry bulb temperature (Tdry)

The left plot in Figure 3.1 (showing the comparison of Tdry of the two psychrometers) shows very good linearity and little scatter (Y= -0.13+1.00X, σy= 0.09 °C).
If we compare Tdry of the LU-psychrometer with the AWS-sensor in the right plot, just to put things in perspective, we see a factor 3 larger scatter. (Y= -0.25+1.02X, σy= 0.27 °C).
Although not shown here, comparison of TdryAW with the TdryAO-psychrometer shows practically the same result, as one would expect reviewing the left plot showing the correspondence between the two psychrometers.
Shown scatter data are 10-minute averages during 7 days at the beginning of the experiment (21/6 - 28/6).
The lower wind speeds (< 1 m/s, represented by "x" in the plot) mostly coincide with lower temperatures and visa versa, due to an usual lower wind speed at night.

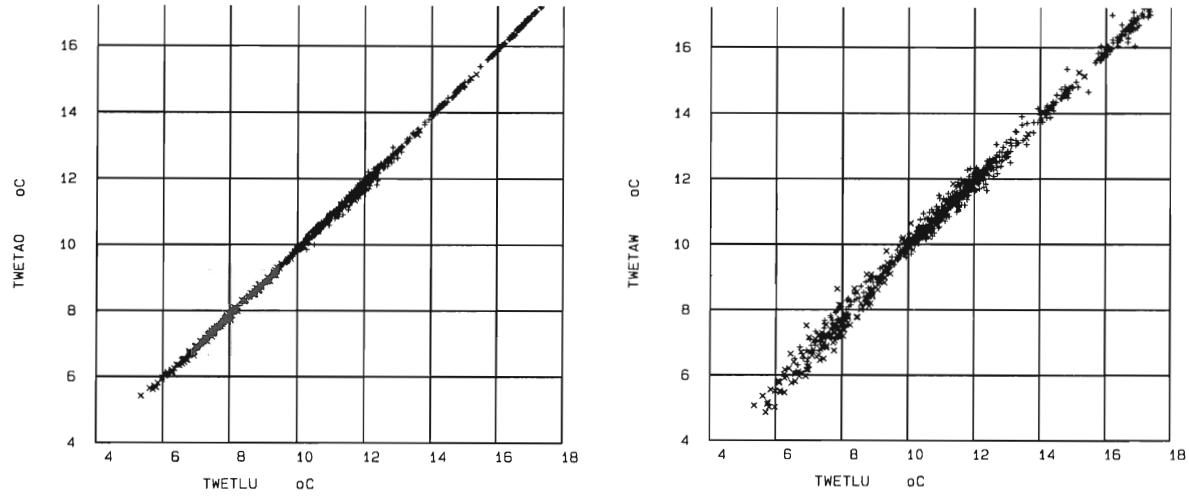

Figure 3.2: *Comparison between wet bulb temperatures; TwetLU with TwetAO (left) and TwetLU with TwetAW (right) for low(x:<1m/s) and high(+:>1m/s) wind speed.*

3.1.2 Wet bulb temperature (Twet)

Again the left plot in Figure 3.2(showing the comparison of Twet of the psychrometers) shows very good linearity and little scatter (Y= -0.15+1.00X, σy= 0.06°C).
But again if we compare TwetLU with TwetAW in the right plot we see a larger scatter; almost a factor 4: (Y= -0.26+1.02X, σy= 0.23°C).
We also notice a slight downward bend of the graph at lower temperatures, which means that the AWS-sensor gives a lower value for Twet than the LU psychrometer.
This effect was consistent during the entire experiment and is discussed in chapter 4.

Although Figure 3.1 and 3.2 show measurements at the beginning of the experiment, during the entire experiment the psychrometer measurements showed comparable results.
The two psychrometers overall showed good similarity, both in time (phase difference) as in value, but there are 2 important notes;

A. Under certain conditions TdryAO deviated 1 à 2 °C from TdryLU (and TdryAW) and considerably lagged behind during 1 à 2 hours.

This occurred approximately on 15 days during the experiment and only in summer between July and September under the following conditions:

- Global radiation between 250 and 550 W/m²
- During the rising temperature in the morning after a few hours of high humidity (95<RH≤100%) or drizzle. (or maybe fog, but this can not be detected by PW-sensor)
- Relative humidity falling and between 90 and 70 %.
- Almost always under dew conditions or when RH was 100% during the night until far (9.00 UTC) in the morning.

This effect might be explained by the high ventilation speed of the AO sensor that wetted the PT-element with moistened air (See figure 3.3 and 3.4)

B. Secondly the average value of TwetAO compared to TwetLU showed a slow decrease of 0.12 °C/month. This was confirmed by a post calibration of the PT-element. Investigation revealed that the hood of the PT-element was not air-tight sealed, so that moisture could wet the inside wiring.
This effect can also be observed in figure 3.3 and 3.4; two months after the start of the experiment TwetAO is ≈ 0.2 °C lower on the average than both TwetLU and TwetAW.

Because of these two facts, in this document the LU psychrometer will be referred to as the reference instrument, against which the performance of the AWS sensors (HMP243 and PT100) is compared.

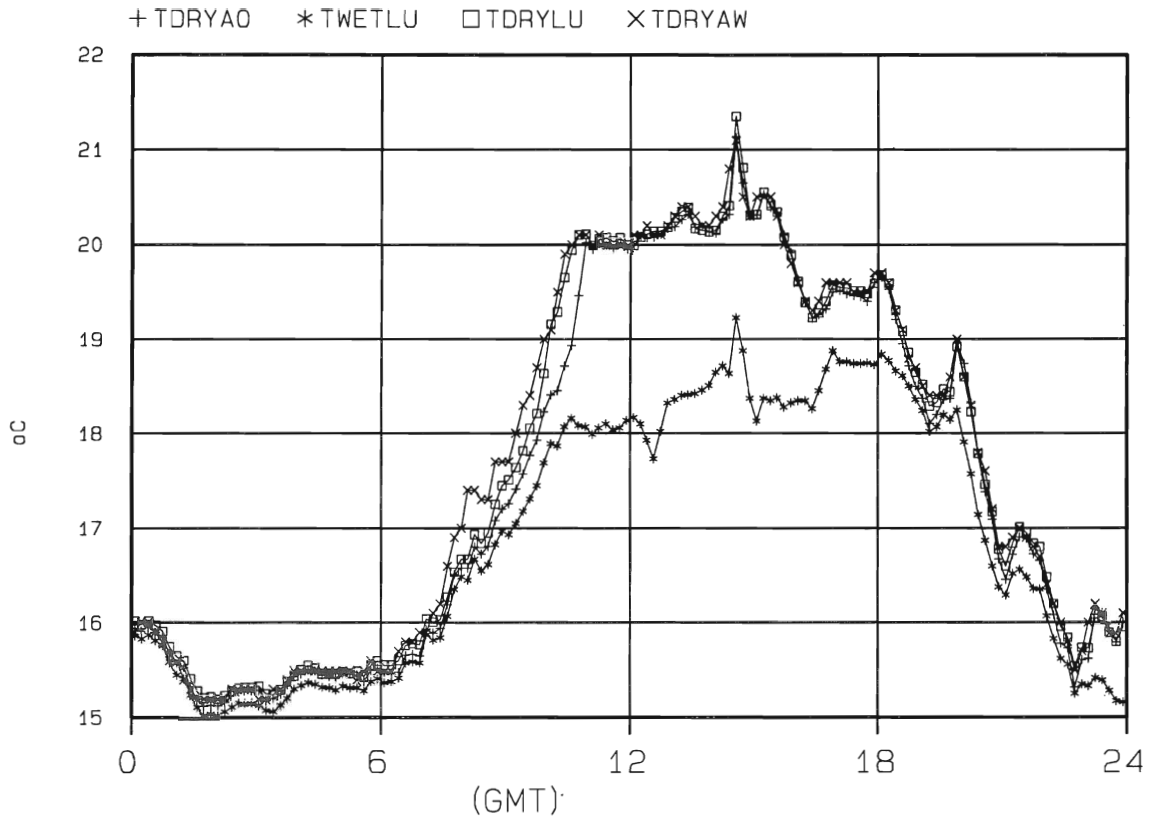

Figure 3.3 *Lagging of TdryAO in a rising slope of the temperature after a dew period.*

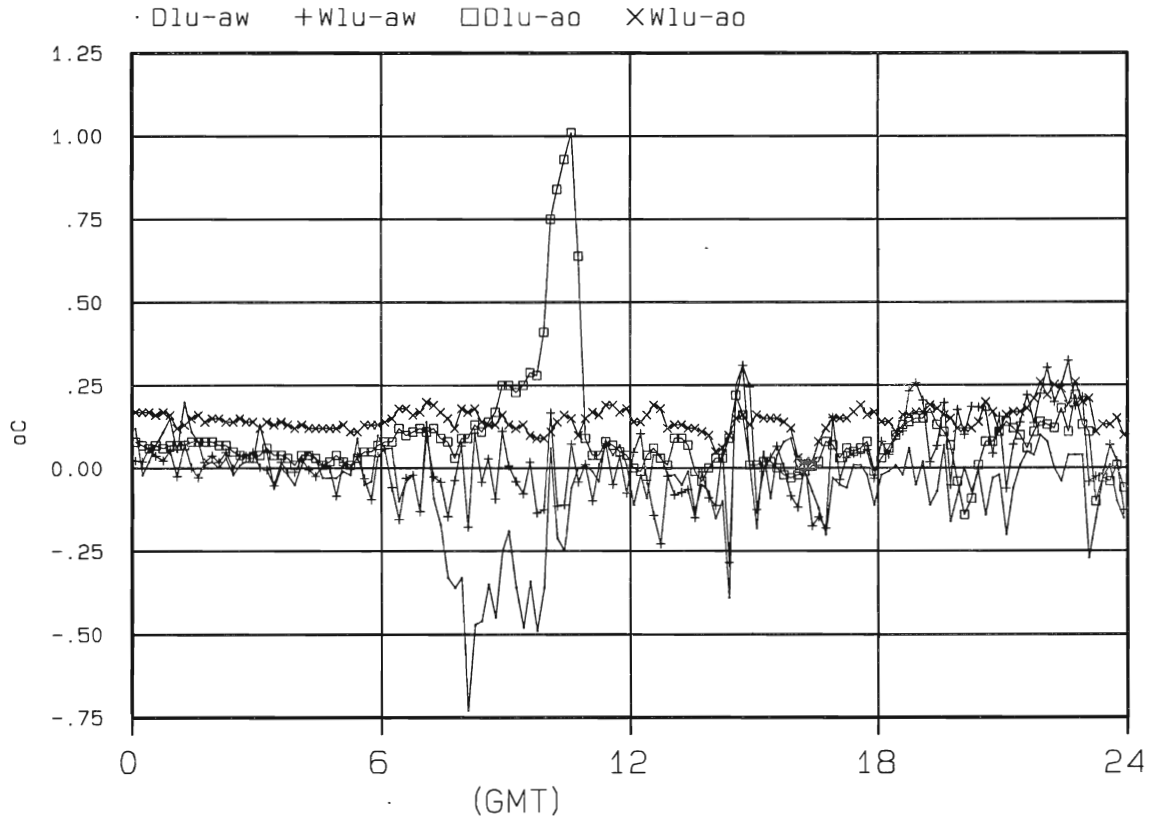

Figure 3.4 *Differences in Dry and Wet bulb temperature of LU-, AWS- and AO sensor, during the same day (8/8/99) as in figure 3.3.*

3.2 Comparison of psychrometer and HMP243/PT100 measurements

In this chapter 3.2 the performance of the humidity sensor HMP243 plus temperature sensor PT100 is compared with the LU psychrometer.
Because this chapter discusses the comparison of two different types of sensors, we first try to exclude errors (timing) other than those from the sensors themselves, in 3.2.1.

From paragraph 3.2.2 on, the actual comparison between the two sensor types is discussed. The scatter diagrams show 10-minute averages from 1/7/99 to 12/11/99.

Dry- and wet screen comparison
A distinction is made between measurements with a wet screen (dew or rain) and a dry screen for a clean comparison.
Dew on the screen influences both temperature and humidity measurements.
A wet screen affects the temperature measurement because evaporation withdraws heat from the measured volume.
The evaporated moisture affects the humidity measurement because it increases the humidity inside the screen.

Night and day comparison
Also measurements during the day and the night are discussed to keep the comparison more clear. The different mechanical aspects of the two sensors have a different effect on the behaviour of the sensor during the day or during the night.
E.g. Note the absence and presence of a ground plate of respectively the HMP243 and PT100 screen and the artificial ventilated psychrometer, in relation to (IR) radiation effects in the night.
Also note the different amount and material of cups used for the KNMI- and Vaisala screens and the artificial ventilated psychrometer, in relation to ventilation and solar radiation effects during the day.

Tdew and Tdry comparison
Preferably we would choose Twet and Tdry as quantities for comparison because they are direct outputs of the reference psychrometer.
But Twet is a calculated quantity for the AWS instrument, derived from Tdry in a KNMI screen and Tdew in another Vaisala screen.
Because the already mentioned different mechanical aspects of these screens, this would blur the comparison for day- and night periods.
Therefore Tdew is chosen as the quantity for humidity comparison, being the direct output of the AWS-sensor and the derived quantity from Tdry and Twet, but nevertheless both measured in one and the same psychrometer.
Tdry is the quantity for the air temperature comparison, being the direct output of the PT100 in the KNMI-screen and the direct output of the dry bulb of the psychrometer.

3.2.1 Reaction speed sensors

Figure 3.5 shows the same September day as Figure 2.4, selected because of the relatively fast changing temperature signal and steep rise at noon. (little precipitation between 10:00–12:00 and at 15:00, broken clouds, global radiation < 400 W/m^2 and FF1.5 ≈ 1.5 m/s, +/– 0.5).

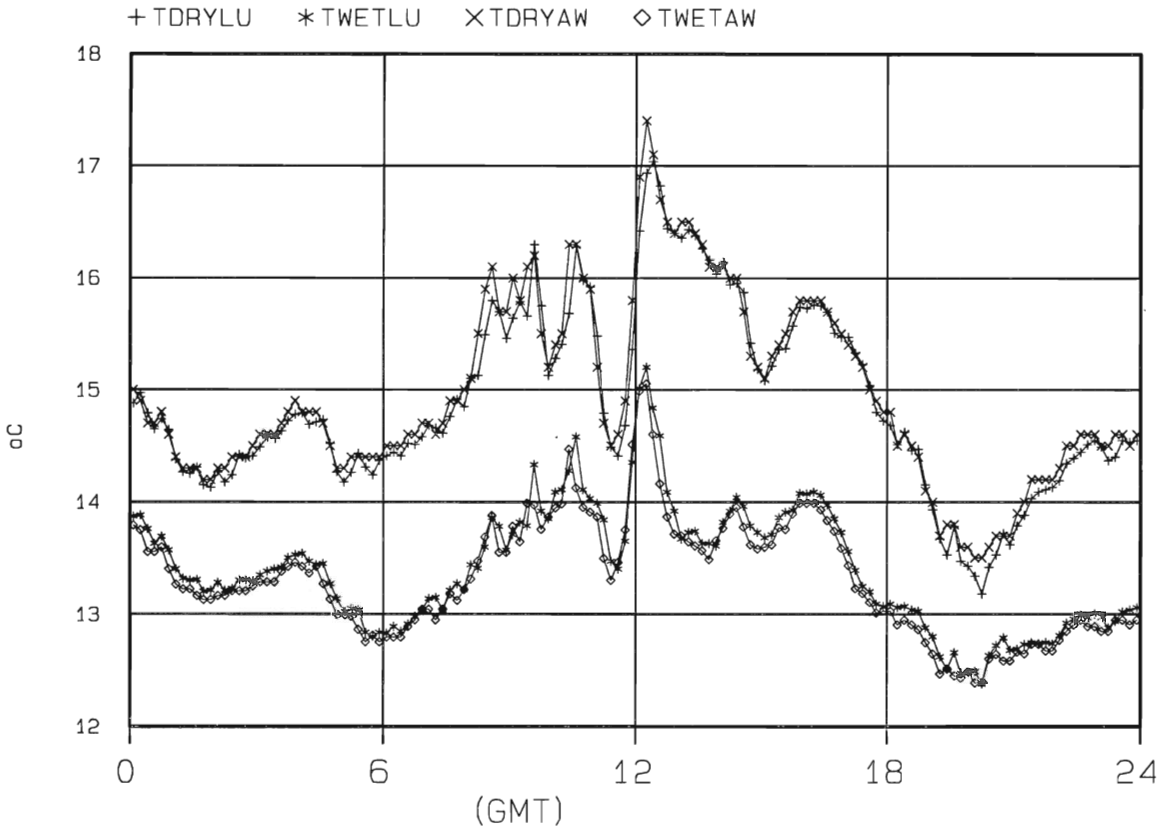

Figure 3.5 *Reaction speed of Tdry and Twet for LU- and AWS sensors on a day with fast changing temperature (broken clouds, precipitation).*

Both TdryAW and TwetAW follow the variations of the LU temperature signals very close. (If we take a closer look we see that TwetAW is a little lower than TwetLU over almost the full 24 hours and that during daytime TdryAW is just a little higher than TdryLU. Both effects are consistent during the entire experiment and will be discussed in chapter 4. Almost without exception both sensors recorded extremes at the same time, so reaction speed seemed similar (at windy conditions). Also rather steep rises in temperature, e.g. round 12:00 in figure 3.5, are recorded at the same time and increase rate. Both rising signals show parallel slopes. Nevertheless in such a steep slope, momentarily differences can occur of more than 0.5°C.
It is obvious that the sensor reaction time depends heavily on the wind speed. Low wind speeds decrease the reaction time of the AWS sensor but have little or no effect on the artificially ventilated LU-sensor.
This effect can be observed in figure 3.5 round 20:00, where TdryAW is lagging behind TdryLU ($\Delta T \approx 0.4°$ C) because the wind speed dropped to less than 0.5 m/s after 18:00. But well ventilated, the reaction speed of the two sensors showed little or no difference.

3.2.2 Tdry comparison under dry conditions

Day time (Qnet >0)

In Figure 3.6 we see that the average TdryAW is significantly higher then TdryLU. The data shows a slight negative correlation between temperature difference and radiation; an average error from 0.2 °C at low levels, to 0.4 °C under sunny conditions (Qnet >500 W/m²).

Over 99% of differences observed between ≈ +1.0 to −0.5 °C.

Note that most of the *"overestimation's"* of TdryAW occurred under calm conditions ("x": FF1.5 < 1 m/s).

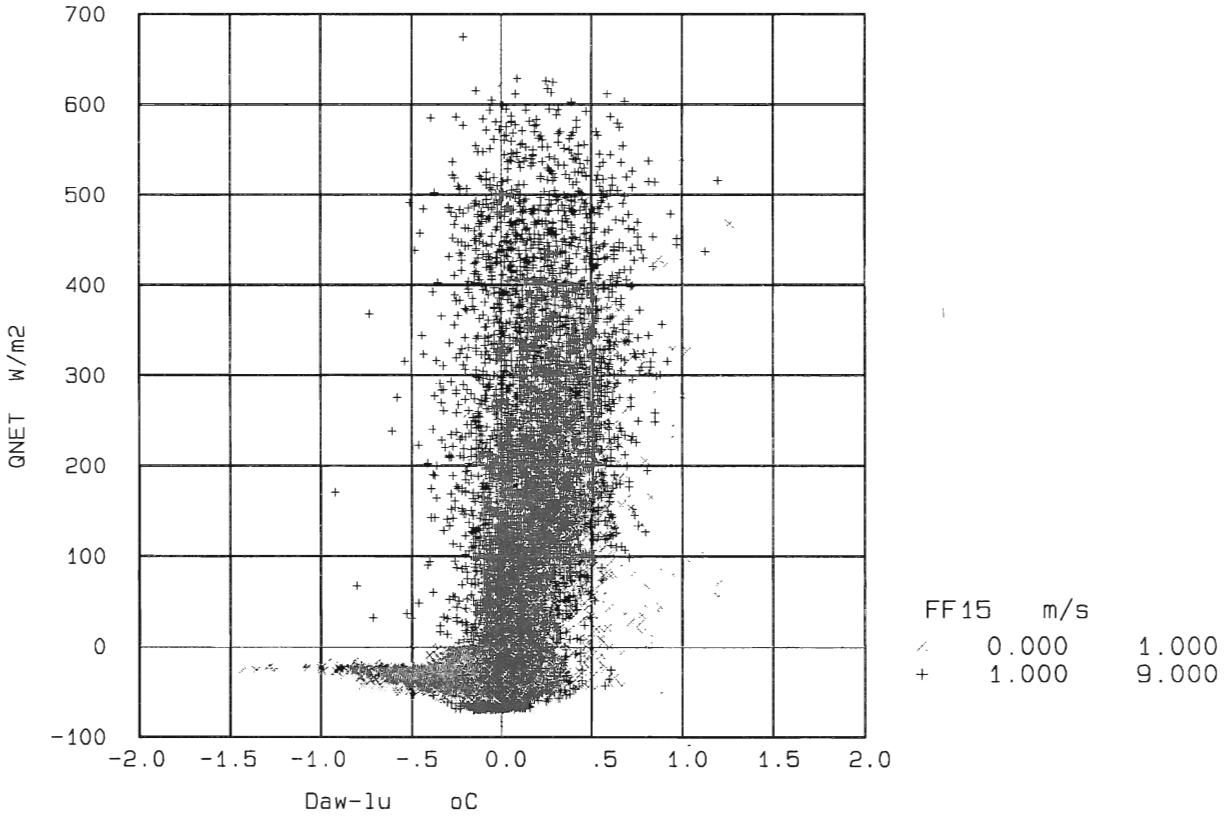

Figure 3.6 *Scatter diagram of TdryAW-TdryLU under **dry conditions** at different radiation levels and for low (x: FF1.5 < 1 m/s) and high (+: FF1.5 > 1 m/s) wind speed.*

An explanation for the *overestimation's* of TdryAW might be;

1. The screen effect that causes a temperature rise inside the screen with increasing radiation level. The fact that almost all *overestimation-extremes* occurred during low wind speed conditions subscribes this hypothesis.
2. Lagging of TdryAW in a falling temperature slope because of the lagging effect of the screen.

A possible explanation for the (fewer) *underestimation's* of TdryAW might be;

1. Lagging of TdryAW in a rising temperature slope.

Night time (Qnet <0)
At night we see some strong *underestimation's* of TdryAW, mainly during low wind speed (common at night).
Over 99% of differences observed between ≈ +0.5 and −1.5 °C.
At wind speeds > 1 m/s the average error is approximately zero (+ or − 0.25 °C).
A lower TdryAW might be caused by radiant heat loss from the surface of the screen at calm nights.

3.2.3 Tdry comparison under wet conditions

Day time (Qnet >0)
In Figure 3.7 we see the difference TdryAW − TdryLU, but now under wet conditions. So dew or rain is detected on the surface of the screens.
We see an average error from +0.1 °C at low radiation levels, to +0.5 °C under sunny conditions.
Relative to the amount of data points we also observe more extreme differences; over 99% observed between ≈ +1.5 and −1.0 °C.
And again extreme overestimation's of TdryAW occurred under low wind conditions.

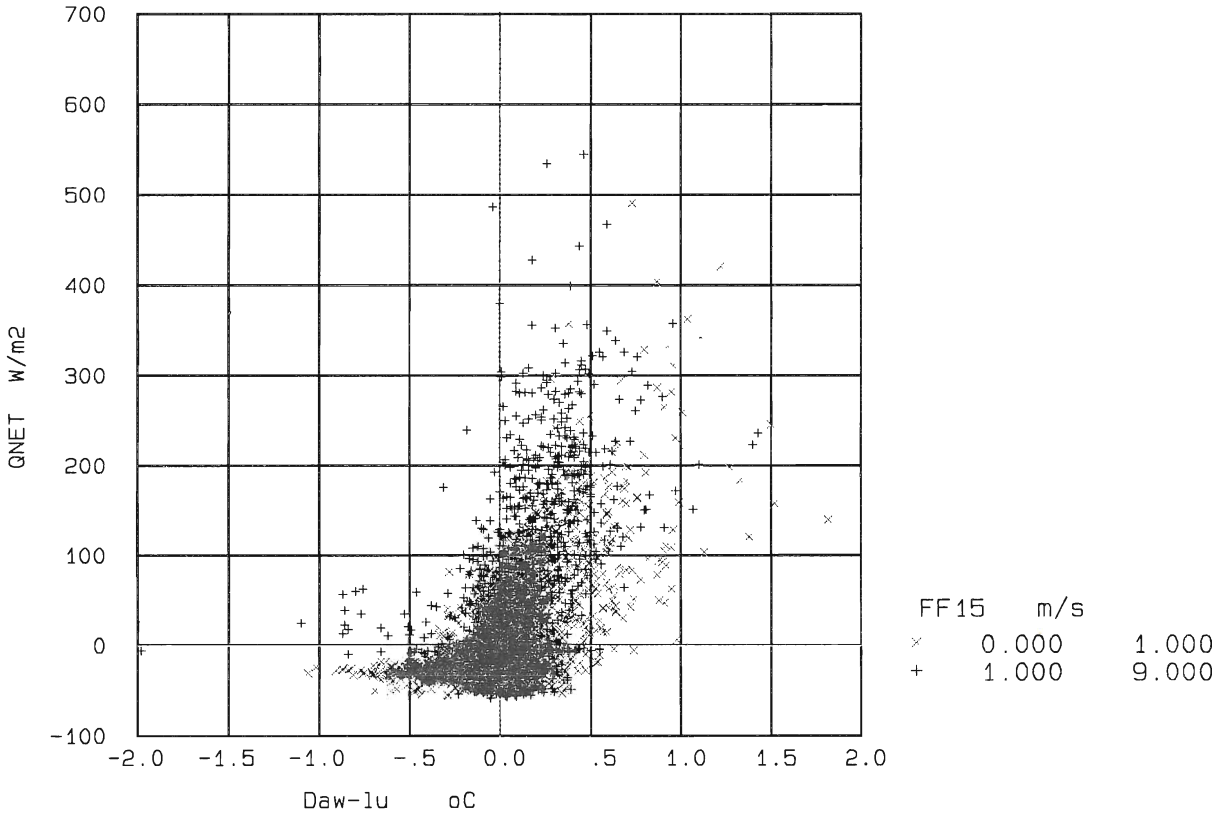

Figure 3.7 *Scatter diagram of TdryAW-TdryLU under* ***wet conditions*** *at different radiation levels and for low (x: FF1.5 < 1 m/s) and high (+: FF1.5 > 1 m/s) wind speed.*

Although the analysis is performed over less data points then in the dry-conditions scatter diagram (Figure 3.6), we observe more underestimation's (between −0.5 and −1.0 °C) of TdryAW, even in absolute number.
This is probably due to a cooling effect caused by evaporation of dew or precipitation on the screen and seems enforced by a chill effect (FF1.5 > 1m/s).
The most extreme overestimation's of TdryAW under wet conditions might also be caused by a lagging effect of the screen because they are mainly observed under calm conditions and during a rising temperature in the morning.

Night time (Qnet <0)
These measurements show more or less the same results as under dry conditions with the exception of an increase of errors under higher wind speeds at Qnet ≈ −10 W/m². The underestimation's are again probably due to the cooling/chill effect and the overestimation's mainly occurred during a wet night (6/11), where both the dry bulb of LU - and AO-psychrometers became wet.

3.2.4. Tdew comparison under dry conditions

Day time (Qnet >0)

In Figure 3.8 we observe rather large differences between TdewLU and TdewAW.

Over 99% observed between ≈ +1.0 and −2.5 °C, so TdewAW is underestimated more extreme and more frequently then TdryAW.

Again the data suggest a slight positive correlation between temperature difference and radiation.

The average error is ≈ −0.3 °C at low levels and −0.8 °C under sunny conditions.

There is no clear relation with wind speed but overestimation of TdewAW tends to occur more at low wind speeds.

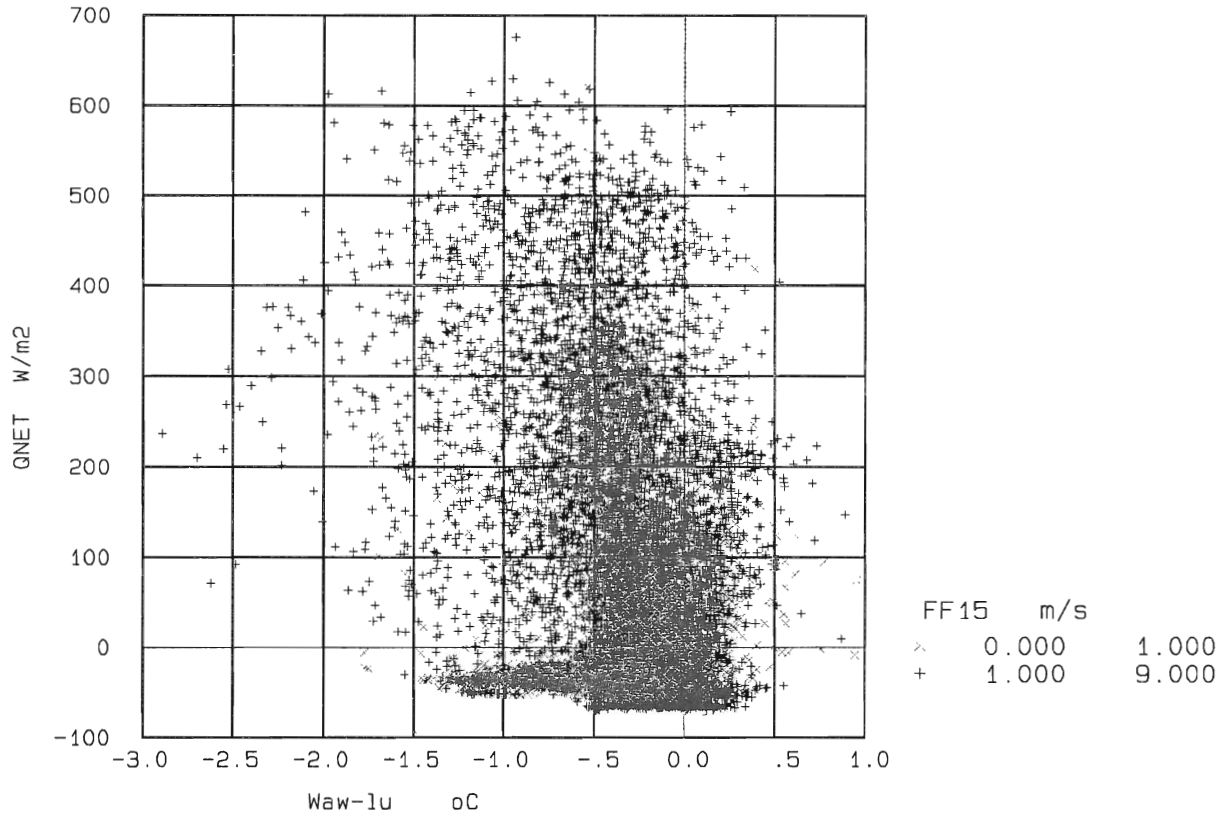

Figure 3.8 *Scatter diagram of TdewAW-TdewLU under **dry conditions** at different radiation levels and for low (x: FF1.5 < 1 m/s) and high (+: FF1.5 > 1 m/s) wind speed.*

Night time (Qnet <0)

At night over 99% of the differences are observed between +0.5 and −1.5 °C.

Again especially at calm conditions we see strong underestimation's of TdewAW.

But also at higher wind speeds (>1 m/s) during clear nights with high radiant heat (Qnet < −50 W/m²) we see rather large underestimation's (>1°C).

3.2.5. Tdew comparison under wet conditions

Day time (Qnet >0)

Figure 3.9 showing the differences of Tdew under wet conditions, shows the same features as Figure 3.8, although extreme underestimation's > 1.5 °C were not observed. Also the wind effect seems stronger under wet conditions. Most of the overestimation's of TdewAW occurred under calm conditions (FF1.5 < 1 m/s).
And like Figure 3.8 the differences are slightly positive correlated with the radiation.

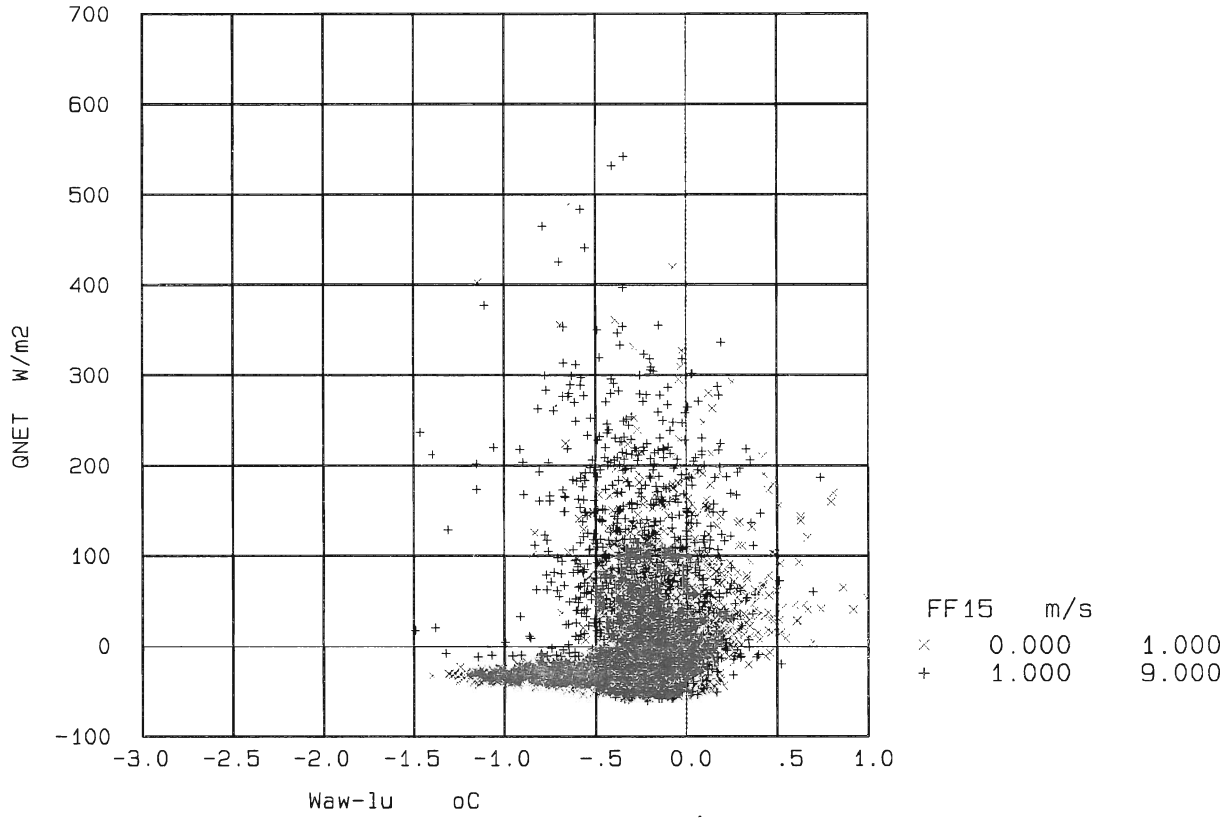

Figure 3.9 *Scatter diagram of TdewAW-TdewLU under* ***wet conditions*** *at different radiation levels and for low (x: FF1.5 < 1 m/s) and high (+: FF1.5 > 1 m/s) wind speed.*

Night time (Qnet <0)

Like under dry conditions, over 99% of the differences are observed between +0.5 and −1.5 °C.
Note the absence of high wind speed data points for Qnet < −50 W/m², which we saw so clearly under dry conditions.
Most likely explanation is that high winds at night will dew cause to evaporate from the screens, so that these wet conditions under high winds at night are mainly caused by precipitation only, instead of precipitation *and* dew.

4. Conclusions and remarks

Having measured during a period of 6 months with a large variety of meteorological conditions, from summer till early frost, we have evaluated the behavior of an AWS humidity sensor. To choose just *one* reference instrument for the evaluation we first compared two psychrometers, one from LU Wageningen (B. Heusinkveld) and one from AO-KNMI, similar to a model that served the Cabauw tower for more than 25 years (Chapter 4.1).
Secondly we compared Vaisala's HMP243 humidity sensor + PT100 (= AWS sensor), with the chosen reference psychrometer (Chapter 4.2).
Considerable differences were measured between the sensors, both in dewpoint temperature (Tdew) as in dry bulb temperature (Tdry).

4.1 Comparison of LU- and AO-psychrometer measurements

The two psychrometers, although quite different in design performed very equally. Both were constructed to prevent two main sources of error in temperature measurements;
1) Screening and isolation of sensors against direct solar radiation.
2) Ventilation to avoid stagnant air to be heated by the radiation shield and to avoid a slow response.
The psychrometers showed very good similarity both for dry bulb temperature (Y= -0.13+1.00X, σy= 0.09 °C), as for wet bulb temperature (Y= -0.15+1.00X, σy= 0.06 °C).
Although the two sensors performed very similar, both in time (phase difference) as in absolute value, there are two important notes;

1. Under certain meteorological conditions Tdry of the AO sensor deviated 1 à 2 °C from Tdry LU (and Tdry AWS), and considerably lagged behind during 1à 2 hours.

This occurred approximately on 15 days during the experiment and only between July and September under specific conditions, described in chapter 3.1.2.
The effect might be explained by the high ventilation speed of the AO sensor that wetted the PT-element with moistened air.

2. Due to a little mechanical failure of the PT-element in the AO psychrometer, the average wet bulb temperature of the AO psychrometer showed a slow decrease of 0.1 °C per month, compared to the average LU wet bulb temperature.

Because of these two facts, the LU psychrometer is referred to as the reference instrument in this rapport, to which the performance of the AWS sensors (HMP243 and PT100) is compared.

4.2 Comparison of psychrometer and HMP243/PT100 measurements

As seen in chapter 3, these sensors showed much less similarity, both in Tdry; (Y= -0.25 +1.02X, σy =0.27 °C) as in Twet; (Y= -0.36 +1.02X, σy =0.23 °C). The scatter is, in relation to the comparison of the two psychrometers, 3x larger for Tdry and 4x larger for Twet.
Especially when Twet dropped below 10 °C, an underestimation (≤ 1 °C) of the AWS-sensor could be observed, consistent during the whole experiment (see Figure 3.2- right).

Because of the mechanically and physically differences between the AWS-sensor and the psychrometer, different phenomena should be taken into consideration for an explanation.

Screen effect
All natural ventilating screens have solar radiation and night cooling effects (G. Levebvre, 1998). Some cup screens show behaviour rather similar to Stevenson screens. Radiation at the screen heats the enclosed volume during the day. And loss of radiant heat cools the screen during the night, especially at clear nights.

Lagging effect
It is obvious that the mechanically aspects of a screen also influence the reaction time of a sensor. Air parcels enclosed by a screen like that of the AWS sensor are "refreshed" slowly at calm conditions. So the reaction time of the sensor depends heavily on wind speed.
Low wind speeds decrease the reaction time of both the HMP243 in the Vaisala screen as the PT100 in the KNMI-screen but have little or no effect on the artificially ventilated LU-sensor.

Level effect
From studies of ground level measurements in Cabauw (F. Bosveld) it is known that under calm conditions (non mixed layers) at night, temperature gradients can occur of ≈0.1°C/0.1 m. Sensors mounted on a slightly higher level above the ground then others could therefore give a higher temperature reading under these conditions.

Advection error
If the wind speed exceeds the ventilation velocity of the psychrometer, air heated by the outer radiation shield could reach the sensor (W.H. Slob, WR-78-1). For this experiment such errors are very unlikely because the wind speed at instrument level never exceeded 6.5 m/s during this experiment.

Tdry comparison

Over 99% of all differences (TdryAWS – TdryLU) observed between +1.5 and –1.5 °C.

On a daily time scale, the difference signal appeared negatively correlated with radiation. Meaning that the AWS-sensor underestimates the temperature at the beginning and end of the night and it overestimates temperature during the day. The difference signal was larger when radiation changed quickly in time. Short wave radiation heats the enclosed volume during the day and long wave radiant heat loss cools the screen during the night (*screen effect*).
Also a slightly negative correlation between [TdryAWS–TdryLU] and Qnet is observed.

Besides the screen effect, two other phenomena play a role here, having opposite effects;
The earlier described *lagging effect* introduces an overestimation of the AWS sensor in the falling temperature slope during the night and an underestimation in the rising slope during the day. This effect is only observed during cloudy days.
Secondly, as the AWS PT100 sensor is mounted on a level less then 10 cm above the LU sensor, overestimation's of the AWS sensor ≤ 0.1 °C can be ascribed to the *level effect* under calm conditions.
Both *lagging-* and *level effect* are fully "overshadowed" by the *screen effect* and the average TdryAWS is significantly higher then TdryLU during the day and lower during the night.

Average overestimation at day time: ≈ 0.2 °C at low radiation levels, to 0.4 °C under sunny conditions. Most extreme overestimation's occurred during calm conditions. This occurred especially during rising temperatures in the morning (often dew on screen).
At night: over 99% of differences observed between ≈ +0.5 and –1.5 °C. Most extreme underestimation's occurred during calm conditions.

Tdew comparison

Over 99% of all differences (TdewAWS – TdewLU) observed between +1.0 and –2.5 °C.

The differences are now positively correlated with the radiation.
TdewAW is underestimated more extreme, and more frequently then TdryAW.
The average error is ≈ -0.3 °C at low radiation levels and -0.8 °C under sunny conditions.
There is no clear relation with wind speed but at low wind speeds overestimation of TdewAW tends to occur more, with rain or dew on the screen. This might be related to hygroscopical properties of the sintered sensor hood.
At night: over 99% of differences observed between ≈ +0.5 and –1.5 °C. Most extreme overestimation's occurred under calm conditions.

Concluding remarks

Seen these results we can draw the conclusion that the AWS-humidity sensor cannot attain the accuracy of the formerly used psychrometers.
The expected accuracy of the AWS dry bulb temperature and dewpoint temperature is typically 0.1 and 0.3 °C respectively. In this comparison we observed differences of some degrees between the reference and AWS-sensor, especially under calm conditions and at night (in particular Tdew).
A possible non-functional heating of the HMP243 cannot explain these differences because it does not affect Tdew or Tdry.

For the determination of humidity and temperature profiles of the boundary layer, as performed in the Cabauw tower, an even higher accuracy is necessary, due to small differences (tenths of degrees) between the different levels. Besides this, the sensors in the tower are exposed to different conditions at different levels and thus errors (lagging, level & screen effect) will be level dependent.

Another aspect is the continuity of time series. In climate research, long time series of continuous temperature measurements are needed. With the eventually replacement of the HMP233 by the new HMP243 it is essential that the behaviour of a new sensor compared to the old one is well known and documented.

I have my doubts about the fact that for the determination of the relative humidity, two sensors are used in two completely different screens with different behaviour under certain meteorological conditions. The temperature measurement in separate screens can lead to unpredictable errors, especially at sunrise and sundown, when one screen is in the shadow of the other.

So according this evaluation the HMP243/PT100 measuring system is not suitable for quantitative temperature and humidity profile measurements or even operational temperature and humidity measurements.

5. Acknowledgements

I hereby want to thank Fred Bosveld and Wim Kohsiek of the Atmospheric Research Division of KNMI for careful reading and valuable comments on earlier versions of this document.
Bert Heusinkveld of LU-Wageningen for lending the psychrometer and supplying very nice wet bulb sleeves.
Alexander Mazee for supplying the AWS data every week.
Foeke Kuik for information on the HMP243 sensor and INSA for setting up the AWS-instruments at the experimental site.

6. Appendix

Calibration curve PT500 dry bulb AO

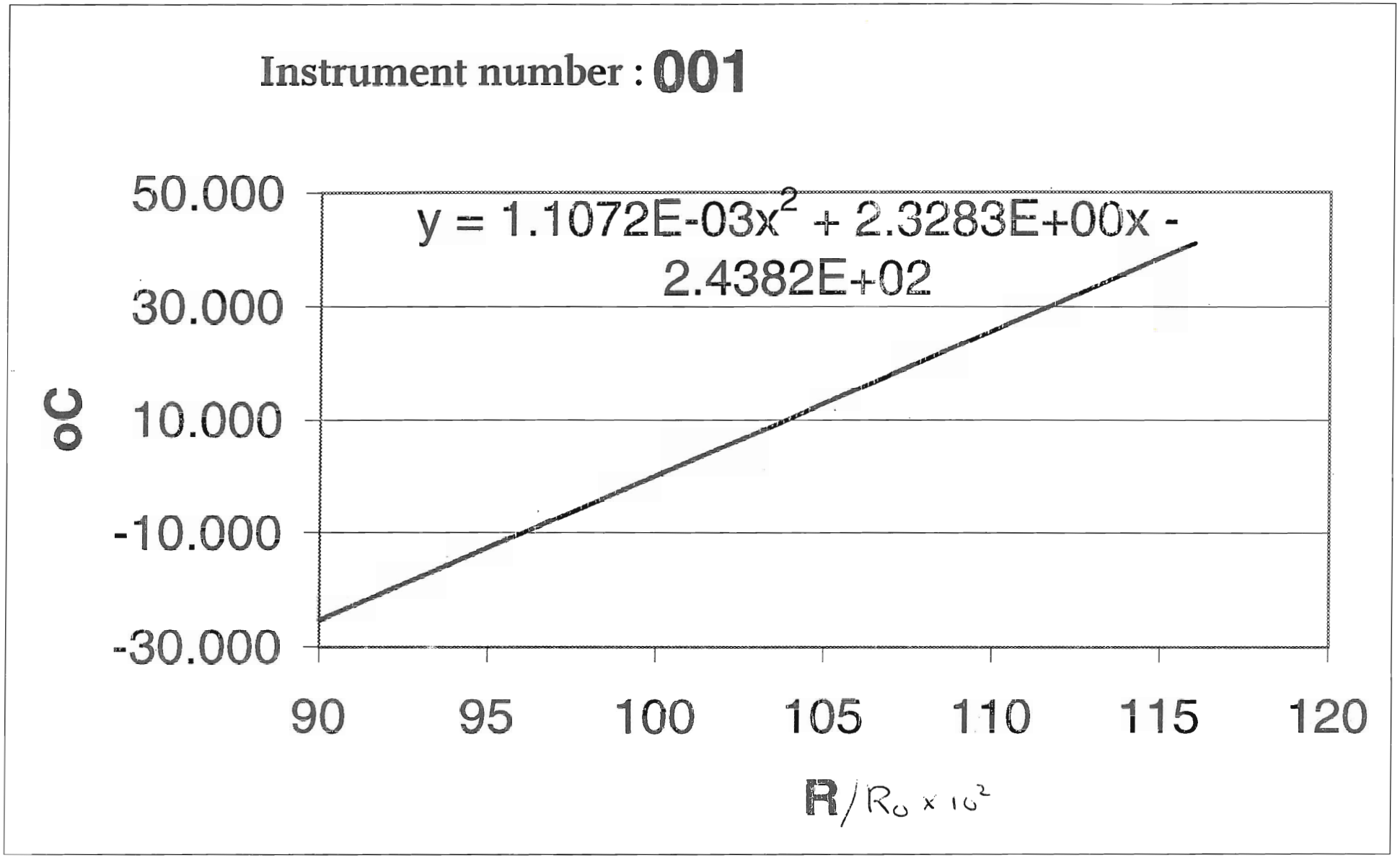

Postadres: Postbus 201, 3730 AE De Bilt

Bezoekadres: Wilhelminalaan 10

KNMI

IJkcertificaat

Datum ijking : 1999-05-07 **IJking geldig tot : 2002-07-07**

INSTRUMENT	:	PT500 sensor
INSTRUMENTNUMMER	:	001
MEETBEREIK	:	- 30 tot + 50 °C
FABRIKANT	:	KNMI
IJKNAUWKEURIGHEID	:	0.05 °C

De temperatuursensor is in een vloeistofbad gekalibreerd door vergelijking met een standaardthermometer.

Merk	:	ASL	-	Tempcontrol
Type	:	F25	-	Pt100
Serienr.	:	1163-21/146	-	SL92 T 169
Certificaatnr.	:	NMI	-	3404653

De volgende correcties gelden :

Temperatuur KNMI in °C		Correctie Instrument in °C
- 15	:	+ 0.135
- 10	:	+ 0.115
- 5	:	+ 0.093
- 0	:	+ 0.072
+ 5	:	+ 0.053
+ 10	:	+ 0.041
+ 15	:	+ 0.024
+ 20	:	+ 0.013
+ 25	:	+ 0.001
+ 30	:	- 0.010
+ 35	:	- 0.026
+ 40	:	- 0.040

Werkelijke temperatuur = Afgelezen temperatuur + Correctie

Hoofd IJklaboratorium

A. van Londen

Calibration curve PT500 wet bulb AO

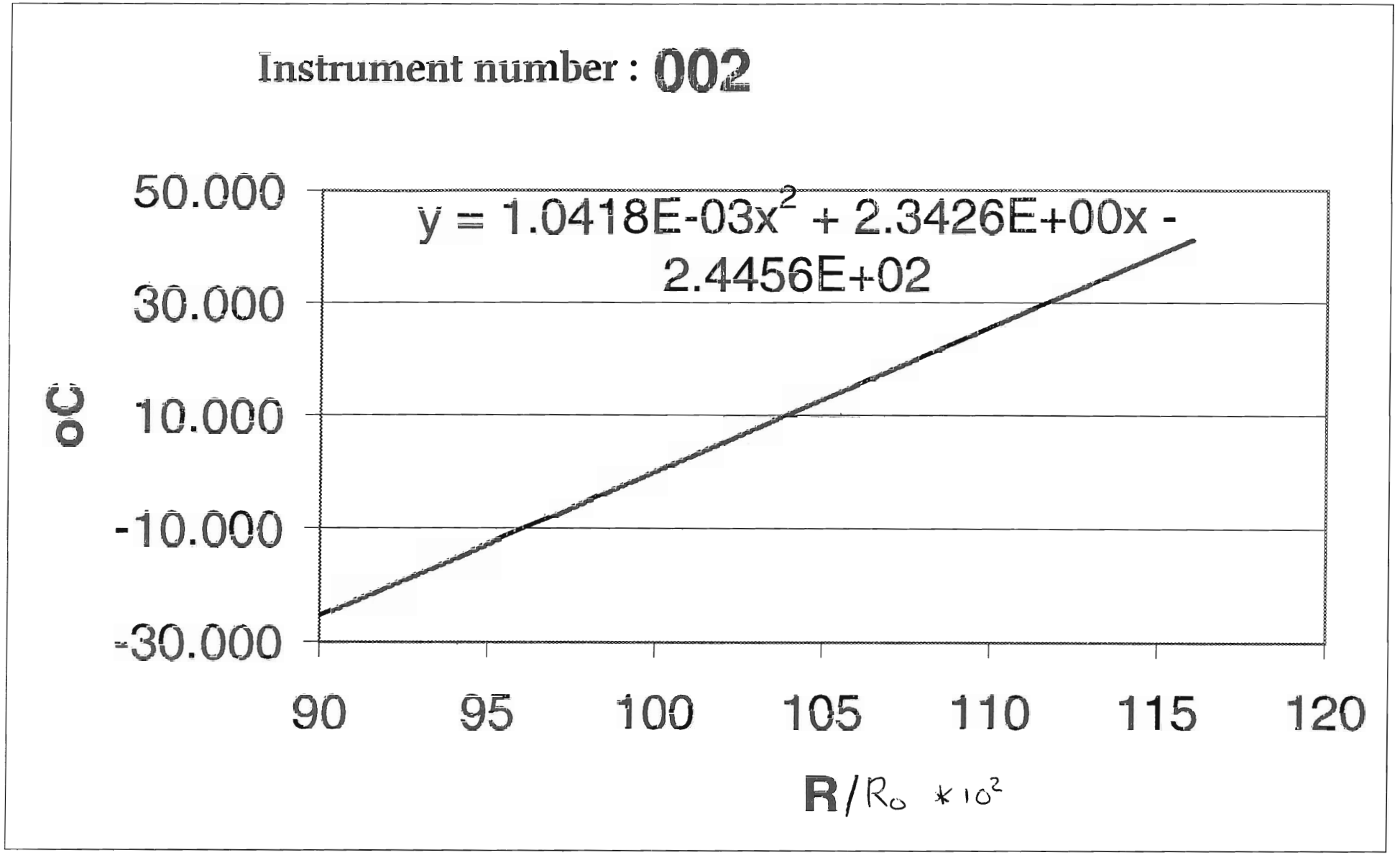

Postadres: Postbus 201, 3730 AE De Bilt

Bezoekadres: Wilhelminalaan 10

KNMI

IJkcertificaat

Datum ijking : 1999-05-07 **IJking geldig tot : 2002-07-07**

INSTRUMENT	:	PT500 sensor
INSTRUMENTNUMMER	:	002
MEETBEREIK	:	- 30 tot + 50 °C
FABRIKANT	:	KNMI
IJKNAUWKEURIGHEID	:	0.05 °C

De temperatuursensor is in een vloeistofbad gekalibreerd door vergelijking met een standaardthermometer.

Merk	: ASL	-	Tempcontrol
Type	: F25	-	Pt100
Serienr.	: 1163-21/146	-	SL92 T 169
Certificaatnr.	: NMI	-	3404653

De volgende correcties gelden :

Temperatuur KNMI in °C		Correctie Instrument in °C
- 15	:	+ 0.171
- 10	:	+ 0.154
- 5	:	+ 0.136
- 0	:	+ 0.119
+ 5	:	+ 0.101
+ 10	:	+ 0.091
+ 15	:	+ 0.079
+ 20	:	+ 0.066
+ 25	:	+ 0.056
+ 30	:	+ 0.043
+ 35	:	+ 0.029
+ 40	:	+ 0.018

Werkelijke temperatuur = Afgelezen temperatuur + Correctie

Hoofd IJklaboratorium

A. van Londen

21.06.050

Calibration curve PT100 Schulze radiometer

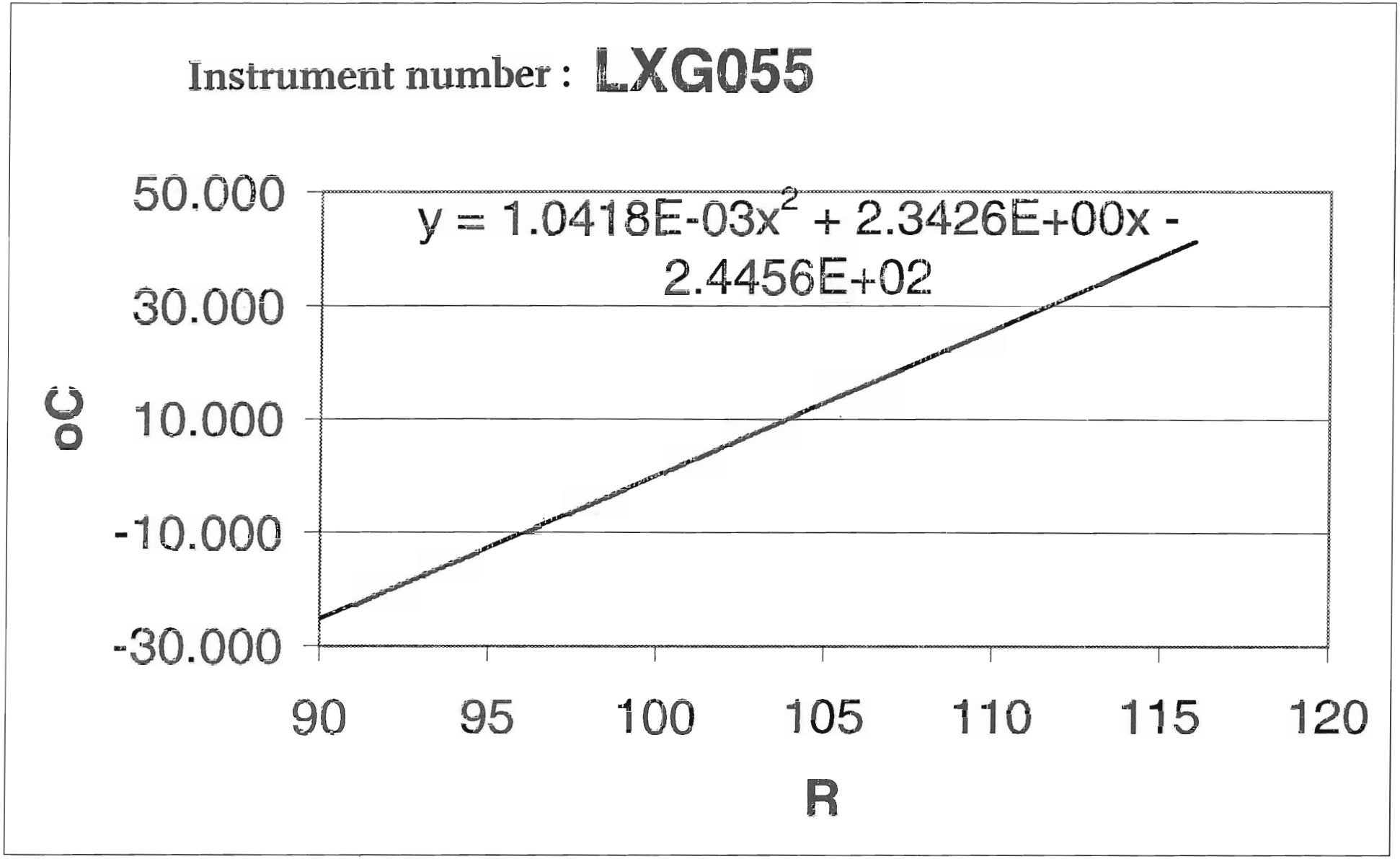

Postadres: Postbus 201, 3730 AE De Bilt

Bezoekadres: Wilhelminalaan 10

KNMI

IJkcertificaat

Datum ijking : 1999-05-07 **IJking geldig tot : 2002-07-07**

INSTRUMENT	:	PT100 sensor
INSTRUMENTNUMMER	:	LXG 055
MEETBEREIK	:	- 30 tot + 50 °C
FABRIKANT	:	KNMI
IJKNAUWKEURIGHEID	:	0.05 °C

De temperatuursensor is in een vloeistofbad gekalibreerd door vergelijking met een standaardthermometer.

Merk	: ASL	-	Tempcontrol
Type	: F25	-	Pt100
Serienr.	: 1163-21/146	-	SL92 T 169
Certificaatnr.	: NMI	-	3404653

De volgende correcties gelden :

Temperatuur KNMI in °C		Correctie Instrument in °C
- 15	:	+ 0.094
- 10	:	+ 0.079
- 5	:	+ 0.065
- 0	:	+ 0.055
+ 5	:	+ 0.041
+ 10	:	+ 0.039
+ 15	:	+ 0.028
+ 20	:	+ 0.024
+ 25	:	+ 0.021
+ 30	:	+ 0.016
+ 35	:	+ 0.009
+ 40	:	+ 0.001

Werkelijke temperatuur = Afgelezen temperatuur + Correctie

Hoofd IJklaboratorium

A. van Londen

LANDBOUW UNIVERSITEIT WAGENINGEN
VAKGROEP METEOROLOGIE
DUIVENDAAL2
7601AP WAGENINGEN

YKRAPPORT YKING : PTA13
GEBRUIKTE YK-PT : TEMPCNTR
DATUM : 6-SEPT-94
DATUM BEREKENING: 24-Nov-94

BEREKENING VAN DE YKFACTOREN VAN DE FORMULES :
T=A+B.R+C.R^2 EN Rt=R0(1+a.T+b.T^2)

IN DEZE SERIE MEE-GEYKTE PT'S :

PTL&N	PTA1	PTA13	PTEP8	PTEP9	PT200
PT202					
PT212	PT242	PT243	PT246	PT247	PT256
PT274					

BEREKENDE KONSTANTEN :

		std. err.
A=	-2.438796 .10^2	0.0085981
B=	2.326442	0.0194428
C=	1.1280033 .10^-3	9.185E-05
R0=	99.976896	0.0040118
a=	3.9259048 .10^-3	2.777E-05
b=	-8.06E-07	7.892E-08

MEETGEGEVENS:

BADTEMPERATUUR	SENSOR WEERSTAND	T ber. - T gem.
0.927	100.346	-0.0007
-10.107	96.016	-0.0022
9.963	103.876	0.0097
19.944	107.772	-0.0032
29.84	111.619	-0.0091
39.932	115.521	0.0054

GEBRUIKT VOOR:	DATUM	OPMERKINGEN

LANDBOUW UNIVERSITEIT WAGENINGEN
VAKGROEP METEOROLOGIE
DUIVENDAAL2
7601AP WAGENINGEN

YKRAPPORT YKING : PT256
GEBRUIKTE YK-PT : TEMPCNTR
DATUM : 6-SEPT-94
DATUM BEREKENING: 24-Nov-94

BEREKENING VAN DE YKFACTOREN VAN DE FORMULES :
T=A+B.R+C.R^2 EN Rt=R0(1+a.T+b.T^2)

IN DEZE SERIE MEE-GEYKTE PT'S :

PTL&N	PTA1	PTA13	PTEP8	PTEP9	PT200
PT202					
PT212	PT242	PT243	PT246	PT247	PT256
PT274					

BEREKENDE KONSTANTEN :

		std. err.
A=	-2.469144 .10^2	0.0011168
B=	2.380961	0.002533
C=	0.8937804 .10^-3	1.197E-05
R0=	99.948889	0.0033439
a=	3.913711 .10^-3	2.315E-05
b=	-6.28E-07	6.58E-08

MEETGEGEVENS:

BADTEMPERATUUR	SENSOR WEERSTAND	T ber. - T gem.
0.927	100.316	-0.0015
-10.107	95.999	0.0006
9.963	103.84	0.0010
19.944	107.724	-0.0001
29.84	111.564	0.0004
39.932	115.47	-0.0003

GEBRUIKT VOOR:	DATUM	OPMERKINGEN

Column description of data base VERGEX,De Bilt comp. of temp. and hum. inst.

0	DAG	-	3	TYDIDENTIFIKATIE		
1	BTIJD	min	3	BEGIN TIJD (GMT)		
2	ETIJD	-	4	EIND TIJD (GMT)		
3	DAGNR	-	3	DAGNUMMER V.A. 1/1+FRACTIE VAN DE DAG (GMT)		
4	CRDATE	day	0	Creation day of current data file		
5	TDRYAO	oC	1	Dry bulb temperature KNMI-AO psychrometer		
6	TWETAO	oC	1	Wet bulb temperature KNMI-AO psychrometer		
7	TDEWAO	oC	1	Dew point temperature from TDRYAO and TWETAO		*
8	RHAO	%	1	Relative humidity from TDRYAO AND TWETAO		*
9	TDRYLU	oC	1	Dry bulb temperature LU psychrometer		
10	TWETLU	oC	1	Wet bulb temperature LU psychrometer		
11	TDEWLU	oC	1	Dew point temperature from TDRYLU and TWETLU		*
12	RHLU	%	1	Relative humidity fron TDRYLU and TWETLU		*
13	THOUSE	oC	1	House temperature		
14	QIN	W/m2	1	Net incoming radiation Schulze		
15	QOUT	W/m2	1	Net Outgoing radiation Schulze		
16	QNET	W/m2	1	Net radiation Schulze		*
17	RDEW	MOhm	1	Resistance of dew sensor		
18	TDRYAW	oC	1	Dry bulb temperature AWS-261 standard hut	[AWS.TRN]	A
19	TWETAW	oC	1	Wet bulb temperature from TDRYAW and TDEWAW		*
10	TDEWAW	oC	1	Dew point temperature from AWS-261 Vaisala*	[AWS.TRN]	A
21	RHAW	%	1	Relative humidity from AWS-261 Vaisala		*
22	SGLO	W/m2	1	Short wave incoming radiation AWS-RAD	[AWS.TRN]	A
23	SDIR	W/m2	1	Short wave direct radiation AWS-RAD	[AWS.TRN]	A
24	SDIF	W/m2	1	Short wave diffuse radiation AWS-RAD	[AWS.TRN]	A
25	FF15	m/s	1	Wind speed at 1.5 m	[AWS.TRN]	A
26	RDUR	s	6	Duration of precipitation	[AWS.TRN]	A
27	GLOBCL	W/m2	1	Clearsky short wave incoming radiation, Raaf model		*
28	PW	-	7	Present weather code	[AWS.TRN]	A
29	QINC	W/m2	1	Incoming total radiation		*
30	QOUTC	W/m2	1	Outgoing total radiation		*
31	P31	-	0	-		
32	p32	-	0	-		
33	P23	-	0	-		
34	P34	-	0	-		
35	P35	-	0	-		
36	P36	-	0	-		
37	P37	-	0	-		
38	P38	-	0	-		
39	P39	-	0	-		
40	P40	-	0	-		
41	P41	-	0	-		
42	P42	-	0	-		
43	P43	-	0	-		
44	P44	-	0	-		
45	P45	-	0	-		
46	P46	-	0	-		
47	P47	-	0	-		
48	P48	-	0	-		
49	P49	-	0	-		